

# CHAPTER-1

## Introduction

---

### **1.1 Friction Stir processing:**

Friction stir processing is a solid state technique which is based on the principle of friction stir welding and used for modified the surface and enhances the mechanical properties of different alloys. Friction stir welding is technique by which two metal plate are joined together with the help of rotating tool. Frictional heat generated between parent metal and tool is used in welding process. The tool is non consumable and different pin profiles like cylindrical, square, threaded cylindrical. This process was invented at The Welding Institute of U.K in 1991 and initially applied to aluminium alloy [1]. The working principle of FSW is very simple. This process consist of special designed tool (non consumable in nature) have two part- one is pin and other is tool shoulder, parent metal which is used for welding. The pin is inserted between the edges of plate and traversed along the line of joint and tool shoulder is used for force applied on the plates. Due to friction between rotating tool pin and parent metal surface friction heat is generated and which is lead to very soft region near the FSW tool and then two pieces of metal are intermixed at the joint by applying pressure there after joint is cooled[2].This joining techniques energy efficient, eco-friendly, and versatile in nature. Particularly it can be used to join high-strength aerospace aluminium alloys and other metallic alloys that are hard to weld by conventional fusion welding. On the basis of FSW a new process known as friction stir processing (FSP) was developed as a tool for microstructure modification [3]. In this case, a rotating tool is inserted in a work piece for localized microstructural modification for a specific property enhancement. This tool causes heavy plastic deformation in the material around the pin. The heating is generated by friction between the tool and the work-piece and plastic deformation of work piece. The localized heating soft the material around the pin and due to combined motions of tool rotation and translation of material move from the front side of the pin to the back side of the pin. Frictional heat generated between tool and work piece is sufficient to secure required amount of plastic deformation of the matrix around the pin of moving tool. Alloys like aluminium, magnesium, copper etc. are most suitable for friction stir processing. FSP increases the super plasticity of material. It modifies the

---

Friction stir processing of AL alloy and effect of number of passes, Sandeep Kumar, DTU 2014

microstructure, increases micro-hardness and enhances mechanical properties like tensile strength, wear behaviour etc. FSP is also used to produce metal matrix composites. For producing composites a groove is made in the plate of an alloy. This groove is filled by ceramic powder then this is processed by a specially designed tool. In processed zone we get ceramic particles reinforced in the metal matrix. Particles are reinforced up to a depth equal to length of pin of tool. The tool has a pin and shoulder. The composites produced by FSP have excellent mechanical and tribological properties as compared to the parent alloy.

## 1.2 Aluminium and its alloys

Different types of aluminium alloy systems are as follows:

- Pure aluminium
- Aluminium-copper alloys
- Aluminium-manganese alloys
- Aluminium-silicon alloys
- Aluminium-magnesium alloys
- Aluminium-magnesium-silicon alloys
- Aluminium-zinc-magnesium and aluminium-zinc-magnesium-copper alloys
- Aluminium-lithium alloys
- Aluminium-plus other elements which do not fall into any of the patterns outlined above.

Aluminium is the backbone of the aerospace industry, which is used to assist with cooking and packaging, help in the manufacture of high grade steel and it is also base for a versatile paint. Pure aluminium is soft, ductile, and corrosion resistant in nature and has a high electrical conductivity. It is widely used for foil and conductor cables. But adding other alloying elements increase the strength of aluminium alloy for other applications. Aluminium is a light and attractive metal exhibiting a high degree of corrosion resistance in normal corrosive environments. It is also soft, hard, easy to weld, difficult to weld, and a host of other seemingly conflicting characteristics. The properties of a particular aluminium product depend on the alloy chosen. The term aluminium refers to a family of alloys. Knowledge of these alloys is the key to the effective use of aluminium. As a major step towards alignment of Aluminium and

Aluminium Alloy compositions on an international basis, most countries have agreed to adopt the 4 digit classification for wrought alloy composition designation. This system is administered by the Aluminium Association (AA), Washington USA, who compile the "Registration record of International Alloy Designations and Chemical Composition Limits for Wrought Aluminium Alloys". The European reference for the alloys will be identified with the preface EN and AW which indicated European Normative Aluminium Wrought alloys. In all other respects the alloy numbers and composition limits are identical to those registered by the Aluminium Association. The first of the four digits in the designation indicates the alloy group in terms of the major alloying elements [4]. Outlined below is the family of aluminium alloys which are readily available commercially:

- 1XXX Aluminium of 99.00% minimum purity and higher
- 2XXX Copper
- 3XXX Manganese
- 4XXX Silicon
- 5XXX Magnesium
- 6XXX Magnesium and Silicon
- 7XXX Zinc
- 8XXX lithium
- 9XXX Unused series

**1XXX series:** - In this group for minimum purities of 99.00% and greater, first digit of four digit indicate major alloy elements and the last two of the four digits indicate the minimum percentage of aluminium. For example, 1060 indicates aluminium purity of 99.60%. The second digit indicates modifications in impurity limits or alloying elements. If the second digit is zero it indicates unalloyed aluminium having natural impurity limits; integers 1-9 indicated special control of one or more individual impurities or alloying elements. For example, 1145 indicates aluminium of 99.45% minimum purity with the second digit 1 indicating special control of Iron and Silicon. Commercially pure aluminium (99.0% pure) is soft, ductile and of little structural value, but it normally contains up to 1.5% impurities; mainly iron and silicon. These have a marked effect on the properties of the metal, so that, with the further hardness acquired during rolling. Commercial purity aluminium has a useful degree of strength

and it is widely produced in sheet form. It is very ductile in the annealed condition, has excellent corrosion resistance and is ideal for use in the food and chemical industries. It is rolled to foil thickness for use in food, confectionery and cigarette packaging and it has even been used for making shaped panels for vehicles where its high elongation was of prime importance for the forming processes involved.

**2XXX to 8XXX series:** -In these groups the last two of the four digits have no special significance but serve only to identify the different alloys in the group. The second digit indicates alloy modifications; if it is zero it indicates the original alloy.

**2XXX series:** -With copper as the principle element, these alloys require solution heat treatment to achieve optimum mechanical properties, which can exceed that of mild steel. This group of alloys with additions such as Pb (X2030) or Pb + Bi (2011) give the best machinability but there is a trend to avoid these additions because of potential scrap contamination. Typical alloys in this group are 2017, 2024, 2014 X2030 and 2011. Generally, these alloys have limited cold formability, except in the annealed condition. These are less corrosion resistance than other alloys; they are therefore generally anodised for protection from aggressive environments. They are also more difficult to weld. Alloys in this family are particularly useful for aircraft and military applications.

**3XXX series:** - The addition of approximately 1% manganese increases the strength by approximately 10 - 15% compared with AA1200, without any major loss in ductility. This non-heat treatable alloy generally finds a wide application where greater strength than 1200 is required without any major loss in corrosion. Major end uses of the common alloys in this range include roofing sheet (3105 + 3103) and vehicle panelling (3103).

**4XXX series:** - Silicon can be added to aluminium alloys in quantities sufficient to cause a substantial lowering of the melting point. For this reason this alloy system is used entirely for welding wire and brazing filler alloys, where melting points lower than the parent metal are required. In themselves these alloys are non-heat-treatable but in general they pick up enough of the alloy constituents of the parent metal to respond to a limited degree of heat treatment.

**5XXX series:** - This series of alloys is non heat-treatable and showing the best combination of high strength with resistance to corrosion (as indicated by its frequent use in marine/sea water applications). This series also shows good weld ability but

when the Mg level exceed 3% there is a tendency for stress corrosion resistance to be reduced, dependent on the temper used and temperature of operation.

Uses: pressure vessels, bulk road and rail vehicles, ships structures, chemical plant.

**6XXX series:** - This group of heat-treatable alloys uses a combination of magnesium and silicon (magnesium Silicate) to render it heat-treatable. These alloys find their greatest strength, combined with good corrosion resistance, ease of formability and excellent ability to be anodised. Typical alloys in this group include 6061, 6063 and 6082 used for building structure applications, and land and sea transport applications.

**7XXX series:** - This group of alloys exhibits the highest strength as far as aluminium is concerned and in many cases they are superior to that of high tensile steels. It is the combination of zinc and magnesium which makes the 7XXX alloys heat-treatable and gives rise to their very high strength. This group of alloys is, however, relatively difficult to fabricate and requires a very high degree of technology to produce. It is mainly used in military applications.

### **1.3 Advantage of the FSP process:-**

- It has the ability to join materials which are difficult to join with fusion welding  
Example 2000 and 7000 aluminium alloys
- Friction stir processing improve the tensile strength and fatigue strength of the aluminium alloy
- The grain size refined by the friction stir processing and modified the microstructure of aluminium alloy and also improves the hardness of AL alloy.
- Improve the super plasticity of the metal by FSP.
- Low distortion in long welds
- No fume, porosity and spatter
- Low shrinkage and Energy efficient
- Non-consumable tool is used
- No filler material wire is required
- No gas shielding for processing of aluminium
- No grinding, brushing or pickling required in mass production

#### **1.4 Limitations of the FSP process:**

- Work-pieces must be rigidly clamped
- Backing bar required
- Keyhole leave behind at the end of each Process

#### **1.5 Application of FSP:-**

##### **1 Casting:-**

- Produced defect free product compare to casting like porosity and microstructural defects
- By friction stir processing of a cast metal product reduce the grain size, and the ductility and strength are increased

##### **2 Powder metallurgy:-**

- Friction stir processing is used to improve the microstructural properties of powder metal objects

##### **3 Fabrication of metal matrix composites(MMC)**

# CHAPTER-2

## Literature review

---

Mishra et al. [5] Studied creation of super plastic in 7075 aluminium by using FSP and they increase the super plastic from  $1 \times 10^{-3}$  to  $1 \times 10^{-1} \text{ s}^{-1}$ . The elongations obtained in multiple passes of 7075 Al are super plastic but in single pass material shows slightly greater elongations. Mohsen Barmouz et al [6] Studied the fabrication of Cu/SiC composites by multi pass friction stir processing and find the grain size of the copper matrix and SiC reduced by increasing FSP passes and by proper interfacial bonding reduces the porosity so enhance mechanical properties and electrical resistivity.

Rebecca Brown et al [7] studied welding of AL alloy 7050-T7451 by FSW, find defects may arise during production of the friction stir welded structure, these defects can be removed by multi pass using same nominal parameters and HAZ hardness and transverse tensile strength, Residual stress reduced and softened region associated with the HAZ becomes wider with increasing number of passes. A.G. Rao et al [8] studied the effect of multi-pass FSP on corrosion resistance of hypereutectic Al–30Si alloy and find by using FSP to cast Al–30Si alloy increased its corrosion resistance and there after Increase FSP passes decreased corrosion rate of alloy due to the reduction of grain and silicon particle sizes and increase in homogeneity of microstructure. Z.Y. Ma et al [9] studied the Super-plastic behaviour and deformations mechanism of various regions in multiple pass FSP AL 7075 alloy and determine increase in super-plasticity, shifting of optimum temperature and strain rate in the central zone in multiple pass compare to single pass. Z.Y. Ma et al [10] studied the Effect of multiple-pass FSP on microstructure modification and tensile properties of sand-cast A356 (Al-Si) alloy and find the Si particles broken by FSP uniformly distributed in the entire processed zones created by multiple-pass FSP, tensile strength and ductility of the transitional zones lower than the nugget zones. Aluminium alloy 6061 is most commonly used in defence sector, automobile sector, aircraft industry and in marine areas due to their light density, high strength and better corrosion properties [11]. Aluminium 6061 has a wide range of mechanical and corrosion resistance properties so it is popular for medium to high strength requirements and has good toughness characteristics. Heat treatable wrought aluminium-magnesium- silicon alloys conforming to AA 6061 are of moderate strength and possess excellent welding characteristics over the high strength aluminium alloys.

But, they exhibit poor tribological properties during extensive use [12]. Zhikang et al [13] studied the effects of processing parameters (rotational speed and duration time) on microstructure, mechanical properties of 6061-T4 aluminium alloy friction stir spot welds and find best appearance of the joint can be obtained at higher rotational speed and longer duration time and tensile strength increase with the increasing rotational speed for a given duration time. Don-Hyun Choi et al [14] studied the Behaviour of  $\beta$  phase ( $Al_3Mg_2$ ) in AA 5083 weld created by friction stir welding at different speeds and determine the  $\beta$  phase precipitated preferentially along grain boundaries after the sensitizing heat treatment. Ehab A. El-Danaf et al [15] studied the Microstructure and mechanical properties of friction stir welded joint of AA6082 and post weld heat treated conditions and find the Welding of AA6082 is softening in the SZ and TMAZ being more significant and welded joints strength and hardness can be partially recovered by PWHT (post weld heat treatment), response of PWHT welded samples at lower welding speeds is more labelled than welded at higher speeds. J.Q. Li et al [16] studied Characteristics of the reverse dual-rotation friction stir welding on AA2219-T6 aluminium alloy and find the defect-free joint welded by the RDR-FSW at the optimum welding condition corresponding SAZ, WNZ, TMAZ, HAZ and BM. Grains in the TMAZ elongated in the direction of the maximum shear stress. Micro structures in SAZ and weld nugget zone were characterized by fine and equiaxed grain structures due to the high temperature and intense plastic deformation, but grain size in the SAZ was larger. Micro structures in the HAZ is similar to BM. D. Rao et al [17] studied the Asymmetric mechanical properties and tensile behaviour of aluminium alloy 5083 friction stir welding joints and find the change in hardness occurred more rapidly at the AS than at the RS. The hardness decreased sharply from the HAZ to the SZ on the AS but this gradient is low on RS. Zhikang Shen et al [18] studied the microstructure and mechanical properties of 7075-T6 aluminium alloy joints joined by refill friction stir spot welding (RFSSW) and find the keyhole of the weld can be refilled successfully, the microstructure of the weld shows variations in the grain sizes in the width and the thickness directions. Defects associated to the material flow can be observed. Overall good mechanical properties can be obtained at lower rotational speed and shorter duration time. H. Bisadi et al [19] studied the FSW used to join sheets of AA5083 aluminium alloy and commercially pure copper and investigated the effects of various process parameters rotational and welding speeds on the microstructures and



mechanical properties of the joints and result show that the ultimate tensile stresses decreased by increasing the process temperature. Increasing of the process temperature Leads to the higher amounts of copper particles diffusion to the aluminium sheet, inter-metallic compositions and numbers of micro cracks. Chaitanya Sharma et al [20] observed the post weld heat treatment techniques applied to welded FSW joints of AA7039 alloy for improve their mechanical properties by modifying the microstructure and result show that by Natural aging homogeneous distribution of fine strengthening precipitates and by artificial and step aging agglomerated spherical strengthening precipitates. Solution treatment with and without artificial aging result show abnormal grain growth across the entire region modified by friction stir welding. Xiuli Feng et al [21] studied the microstructure of the stir zone in submerged friction stir processed 2219-T6 aluminium alloy and result show that in stir zone grain size order of magnitude less than the base metal and the area fraction of ultra-fine grains increases as the tool rotational speed decreases. The dominant effect of stir zone softening during submerged (Accelerated cooling) FSP of 2219-T6 is the formation of incoherent equilibrium  $\theta$  precipitates from the base metal  $\theta'$  precipitates. Q. Zhang et al [22] studied Al and TiO<sub>2</sub> powders were used to fabricate in situ Al composites via multiple pass friction stir processing (FSP) and due to reaction between Al and TiO<sub>2</sub>, Al<sub>3</sub>Ti and Al<sub>2</sub>O<sub>3</sub> product were formed. Ultrafine grain sizes of particle were formed by FSP cooling and improve tensile strength of processed part. C. Maxwell Rejil et al [23] studied the different volume ratio of powders TiC and B<sub>4</sub>C used to make hybrid surface composite layer with aluminium alloy AA6360 by making groove on the aluminium plate, filling groove TiC and B<sub>4</sub>C and using FSP. Result shows that improve the wear resistance of aluminium alloy of grade 6360. H.L. Hao et al [24] studied the Effect of welding parameters on microstructure and mechanical properties of friction stir welded joint Al–Mg–Er alloy and find that FSW produced a fine equiaxed grain structure in the NZ and size of the grains in the NZ increased with increasing the rotation speed or decreasing the welding speed. The hardness of the NZ decreased with increasing the rotation speed up to 800rpm thereafter not reduced further. The hardness of the nugget zone increased with increasing the welding speed from 100 to 200 mm/min. H. Badari-narayan et al [25] studied the effect of pin geometry (cylindrical and triangular) on the hook formation, cross- tension strength, and failure mode of friction stir spot-welded joint of 5083-O aluminium alloy and find that the triangular-shaped pin formed finer

grain structure in the vicinity of the weld keyhole compared to the cylindrical pin. Under the same process condition the cross-tension strength of welds made with the triangular pin is twice than the welds made with the cylindrical pin. Magdy M. El-Rayes et al [26] modify the micro-structural and mechanical properties of 6082-T6 Aluminium Alloy by FSP at constant rotational speed and different traverse speeds and determine by Increasing the traverse speed reduces the second phase particle Size so increases the mean hardness and UTS of the stir zone. Khaled J. Al-Fadhlah et al [27] studied the effect of overlapping percentage on micro-structural evolution and mechanical properties on multi-pass friction stir processed aluminium alloy 6063. K. Elangovan et al [28] studied the influence of five different tool profile (straight cylindrical, tapered cylindrical, threaded cylindrical, triangular and square) and three different tool rotational speeds (1500,1600,1700) rpm on the formation of friction stir processing zone in AA2219 aluminium alloy and determine the square pin profile tool produced defect free FSP region, irrespective of all rotational speeds and better tensile properties obtained at 1600 rpm by conducting fifteen experiments on AA 2219 aluminium alloy and micro hardness of joint is maximum corresponding to square pin profile at 1600 rpm. V. Balasubramanian et al [29] studied the effect of tool pin profile and shoulder diameter on the FSP zone formation in AA6061 aluminium alloy and find that the square pin profiled tool produced defect free FSP region, irrespective of shoulder diameter of the tools and tool with 18 mm shoulder diameter produced defect free FSP region, irrespective of tool pin profile and obtain superior tensile strength. F. Nascimento et al [30] studied the in-volume FSP (VFSP) (modification of the full thickness) and the surface FSP (SFSP) (modification of the surface of processed materials up to 2mm depth) on the material of aluminium alloys AA7072-T6 and AA5083-O with different tool geometries. P. Vijayavel et al [31] studied the influence of shoulder diameter to pin diameter (D/d) ratio on tensile strength and ductility of friction stir processed LM25Al -5% SiC metal matrix composites and determine the tool of D/d ratio 3 is optimum comparison to other D/d ratio of tool and he obtain defect free micro and macrostructure in FSP region at D/d ratio 3, maximum tensile strength (192 MPa) and micro-hardness (112 HV) obtained because breakups of SiC particles to fine and equal size, even distribution of SiC reinforced particle in the Al matrix enabled by the optimized frictional heat generation by the shoulder contact.

# CHAPTER-3

## Experimental Procedure

---

### 3.1 process parameters:-

Friction stir processing is a method by which we improve the mechanical properties of metal through intense heating and local plastic deformation. In multi pass tool locally manipulates the microstructure (produce homogeneous, equiaxed and fine grains) by imparting a high level of energy in the solid state without change in phase so that it improves the mechanical properties. From literature reviews and trial work it has been found that many factors affect tensile strength like rotational speed (N), transverse feed rate (F), tool profile, no. of passes. Process parameters rotational speed (N), transverse feed rate (F) and tool pin profile affect the heat generation and distribution of plastically deformed fine grain particles in aluminium alloy matrix and this after influences the tensile strength of the specimen. Past study shows that if rotational speed is less distribution is not uniform and if it is high then defects may be produced like tunnel defect due to excessive turbulence. Square shaped pin tool shows the better distribution of fine grain in aluminium matrix. The rotational speed and traverse speed are fixed after numbers of trials were processed and we obtain optimum traverse and rotational speeds are 25 m/min and 1600rpm. The tool pin profile and D/d ratio are fixed based on the literature review. We obtain maximum tensile strength at D/d ratio 3 and square pin profile produced defect free FSP region, at 18mm shoulder diameter of the tool. Now select the process parameters are shown in table:

Table-1 processing parameters

Rotational Speed (N) (Rpm)	Feed rate (F) (mm/min)	Tool pin profile (T)
1600	25	Square

## **3.2 FSP Tool preparation:-**

### **3.2.1 Selection of tool material:-**

Friction stir welding and processing (collectively referred to as friction stirring) is not possible without the non-consumable tool. The tool produces the thermo mechanical deformation and work piece frictional heating necessary for friction stirring. During the tool plunge, the rotating FSP tool is forced into the work piece. The friction stirring tool consists of a pin or probe, and shoulder. Contact of the pin with the work-piece creates frictional and deformational heating and softens the work-piece material; contacting the shoulder to the work-piece increases the work-piece heating, expands the zone of softened material, and constrains the deformed material. For Al alloys mostly Hardened H-13 tool steel material is selected [7, 9, 26]. Other tool material which can be used for FSP are high speed steels (HSS) [13], high carbon high chromium steel (HCHCr) [23], Cermet tool [22]. H-13 is chromium, molybdenum, vanadium hot work tool steel which is characterized by high harden-ability and excellent toughness. The molybdenum and vanadium act as strengthening agents. The chromium content assists H-13 to resist softening when used at high temperatures. H-13 offers an excellent combination of shock and abrasion resistance, and possesses good red hardness. It is capable of withstanding rapid cooling and resists premature heat checking. H-13 has good machine ability, good weld-ability, good ductility, and can be formed by conventional means. Hardness of tool is 54 HRC. Tool geometry is the most influential aspect of process development. The tool geometry plays a Critical role in material flow and in turn governs the traverse rate at which FSP can be conducted. The Tool has two primary functions: (a) Localized heating, and (b) Material Flow

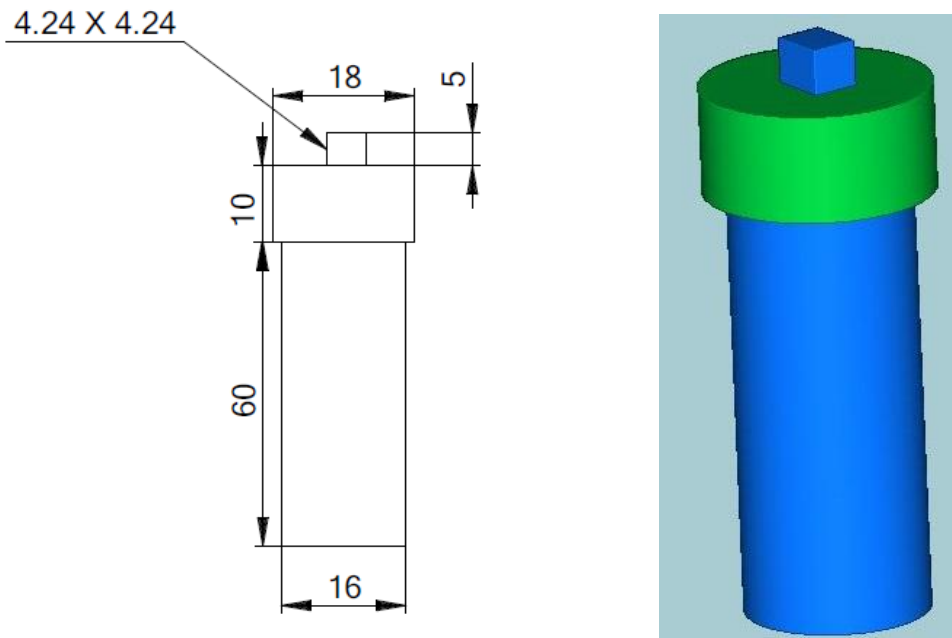
In the initial stage of tool plunge, the heating results primarily from the friction between pin and work-piece with some additional heating results from deformation of material. The tool is plunged till the shoulder touches the work-piece. Due to friction between shoulder and work-piece results in the biggest component of heating. From the heating aspect, the relative size of pin and shoulder is important, and the other design features are not critical. The shoulder also provides confinement for the heated volume of material.

### 3.2.2 Tool Geometry

We select the H-13 tool material, square pin profile tool hardened up to 54HRC.

Table- 2 Composition of H-13 tool

Carbon (C)	Silicon (Si)	Molybdenum (Mo)	Magnesium (Mg)	Vanadium (V)	Phosphorus (P)	Sulphur (S)
0.32- 0.45	0.8-1.2	1.1-1.75	0.2-0.5	0.8-1.2	0.03	0.03



Square pin tool (Sketch and CAD model)



**Before Processing**



**After Processing**



Figure No. 1 (Square pin profile tool)

- Shank diameter 16mm
- Shoulder diameter 18mm
- Pin length 5mm
- Pin profile square

For this study we have chosen figure number four square pin profiles tools. The tools used for the study are shown in -1

### **3.3 work-piece preparation:-**

#### **3.3.1 Selection of work-piece material:-**

The aluminium alloy (grade 1050) of plate dimensions 220mm length, 100mm width and 10mm thickness is select for friction stir processing on milling machine. This grade of aluminium has moderate strength, excellent corrosion resistance, excellent workability, high ductility, highly reflective finish and high thermal and electrical conductivities. It is generally used for chemical and food industry equipment, light reflectors and strips for heat exchangers and Cable sheathing. Its major alloy elements are Iron and silicon.

Table- 3 Chemical composition of aluminium alloy 1050 (mass fraction, %)

Fe	Si	Cu	Mg	Mn	Zn	Ti	Al
0-0.4	0-0.25	0-0.05	0-0.05	0-0.05	0-0.07	0-0.05	Balance

#### **3.3.2 Procedure for preparation of work-piece:-**

1. Cutting of work piece of dimensions (240mm length, 100 mm width and 10mm thickness) from AA1050 Aluminium plate with the help of power hacksaw.
2. Drill the two hole of 10mm diameter at location [(35, 50) mm and (205, 50) mm] on the work-piece with the help of drilling machine.
3. We fixed the work-piece on the table of milling machine with the help of fixtures.



Figure no. 2 FSP specimen plate

### **3.4 Processing Methodology:-**

Non-consumable tools made of H-13 steel with square pin profiles were used to perform the friction stir processing, while the shoulder diameter was 20mm and the pin length and edge were 5 mm and 4.24mm respectively. The shoulder tilt angle was fixed at 2°. Experiments were carried out on a vertical milling machine of capacity of 5 HP. Surface was cleaned by acetone before performing the processing. One pass, two pass, three pass and four pass processed on the work-piece at different locations with the help of H-13 square pin profile tool on the milling machine. Experiments were performed at various parameters according to design matrix shown in table no-1. Figures showing different steps of experimentation:



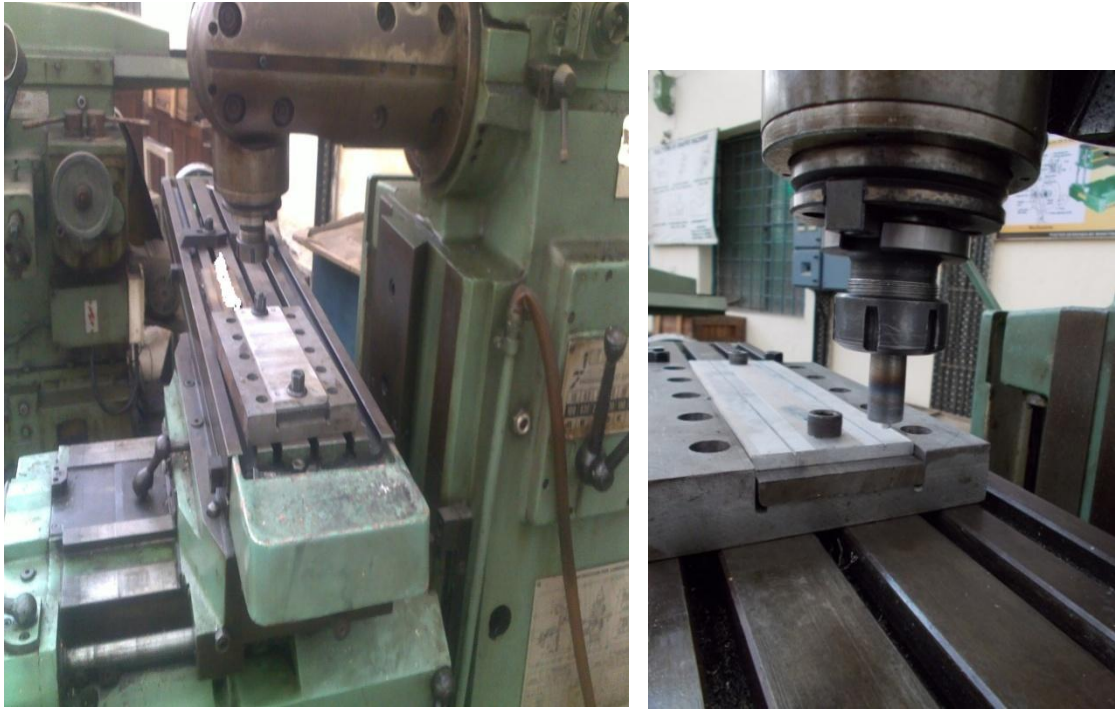


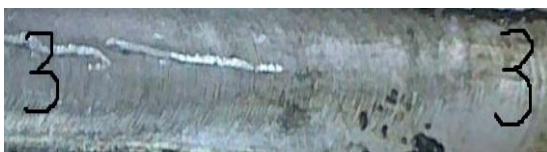
Figure No. 3 Friction stir processing on vertical milling machine



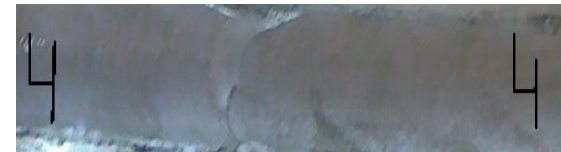
One pass



two pass



Three pass



four pass

Figure No. 4 Friction stir processed zone of different passes

### **3.5 Sample preparation for different testing from friction stir processed plate:-**

#### **3.5.1 Microstructure observation:-**

##### **3.5.1.1 Sample preparation:**

The microstructure and properties of samples varied along the surface to centre line of processed part. Therefore, in order to maintain the uniformity in microstructure, all samples were taken from the central region of processed part.

- Cut the sample from central portion of processed part with the help of wire electric discharge machine.
- Mounting the sample in Bakelite power with the help of mounting machine (simplimet 1000)
- This way we prepared 5 sample



Figure No. 5 Microstructure sample mounting machine

##### **3.5.1.2 Polishing of samples:-**

The sample were polished using different grade of emery paper with progressively coarse to finer one (320, 400,600,800,1000,1200,2000 grits). After completing the paper polishing, the samples were fine polished on rotating disc cotton cloth with alumina powder. Finally the samples were cleaned using ethanol as the cleaning with water not sufficient to remove surface contaminants. The grain structure was revealed

by subsequent etching solution Kellers etch (Distilled water 190 ml, Nitric acid 5 ml, Hydrochloric acid 3 ml, Hydrofluoric acid 2 ml) impression time 10-30 second.



Figure No. 6 Sample fine polishing machine



Figure no. 7 samples for microstructure observation

### 3.5.1.3 Optical microscopy (OM):-

A OLYMPUS-MI optical microscope (Olympus Opto Systems India Private Limited) equipped with the image analysis software, a camera and a computer was used for the OM observation and quantitative measurement of microstructure features. A software application was used to acquire images from camera and to perform image analysis.



Figure no. 8 Setup for microstructure observation

### 3.5.2 Tensile test samples:-

The tensile specimens were taken from the processed surface along the FSP direction and made as per ASTM: B557-06 standard by Wire cut Electrical discharge machining to the required dimensions. The schematic sketch of tensile specimen is shown in Figure 5

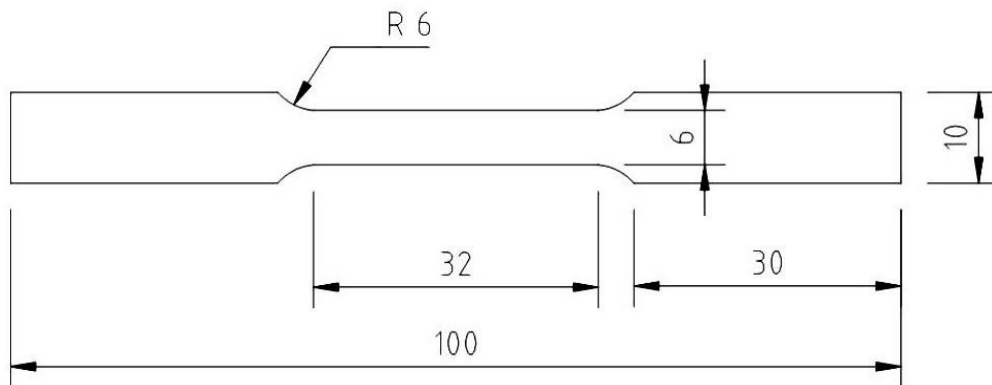


Figure No. 9 Schematic sketch of tensile specimen tested at room temperature

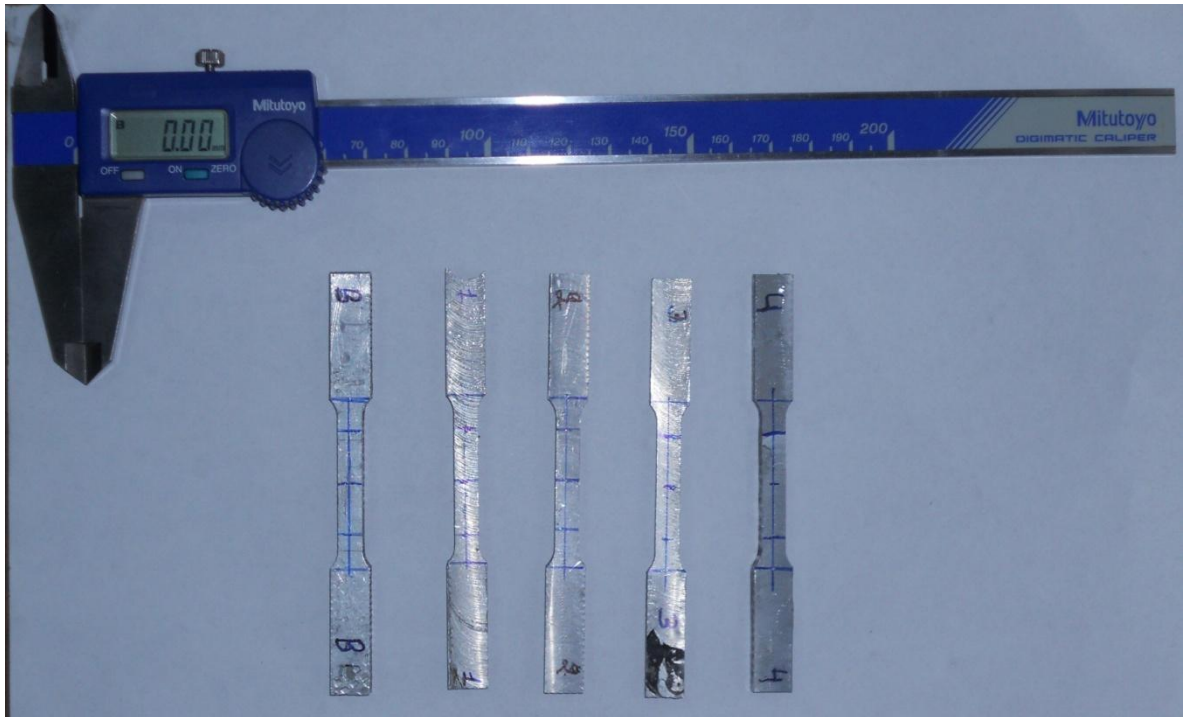


Figure No. 10(a) Tensile specimen before testing



Figure No. 10(b) Tensile specimen after testing



Figure No. 11 Tensile testing machine

The tensile test was conducted with the help of a computer controlled universal testing machine (Tinius Olsen) H50KS strain rate 1mm/min at room temperature (25°C). Ultimate tensile strength and percentage elongation were recorded. Two tensile samples were made from each processed pass. The average of two sample testing data was reported.

### **3.5.3 Wear test:-**

#### **3.5.3.1 Step for preparation of wear sample:-**

- Cutting the 10 mm diameter sample from processed AA1050 Aluminium plate at centre line of one pass, two pass, three pass and four pass with the help of wire electric discharge machine.
- From each processed part four samples are cut and total twenty samples are cutting.

- Drill 5 mm hole on back side of the sample up to depth 5mm with the help of drilling machine.
- Stick 10mm diameter mild steel pin and processed wear sample with the help of Araldite tube and keep it for drying up to two days.
- Flat the top surface of the sample on the surface grinding machine.
- This way we prepared 20 samples.



Figure No. 12 Samples for wear test

### 3.5.3.2 Wear testing operation:-

The sliding test carried out using pin-on-disc machine (model TR 20 LE, manufactured by ducom, Bangalore, India). Insert the specimen pin inside hardened jaw and clamp to specimen holder, set the specimen height above the wear plate and tighten the clamping screws on jaws to clamp specimen pin firmly. Set required wear track radius by moving the sliding plate over graduated scale on the base plate and tighten all six no of clamping screws. Pin of 10 mm diameter wear made to slide against EN-24 material disc of hardness 55 HRC and diameter 160 mm. The track radius kept constant at 100mm, disc speed was maintained at 261 rpm resulting in sliding velocity of 1.5 m/s and constant load 40N applied on each materials. The wear track diameter and disc speed were kept constant during the entire experiment. Frictional force in kg and cumulative wear loss in mm measured from sensor output as a function of time. The wear rates of the pins, defined as the cumulative wear suffered by the pin per unit sliding distance per unit load, were calculated from the cumulative data. The worn

samples surfaces were cleaned by acetone and examined under the scanning electron microscope.

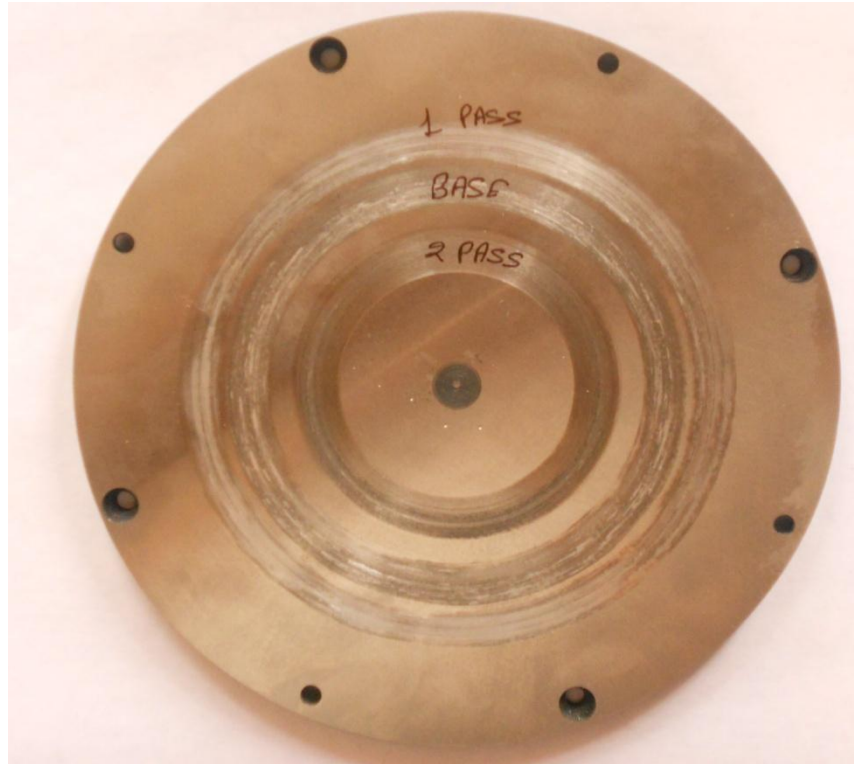


Figure No. 13 sample disc for wear test

**The specifications of the machine are as follows:**

Pin diameter: 4, 6, 8, 10, 12 mm

Disc size: 165 mm diameter and 8 mm thickness

Disc material: EN-24 hardened to 55 HRC

Disc rotation speed: 200 to 2000 rpm continuously variable with digital tachometer

Frictional force: 0 to 200N digital read out with recorder output

Sliding speed: min 0.5m/s to max 10 m/s

Normal load: 1N to 200N

Wear range: -2mm to 2mm

Wear track diameter: min 50mm to max 100mm





Figure No. 14 Wear testing machine

# CHAPTER-4

## Microstructure and Mechanical properties

---

### 4.1 Microstructure:-



Figure No. 15 (a) Microstructure of base material

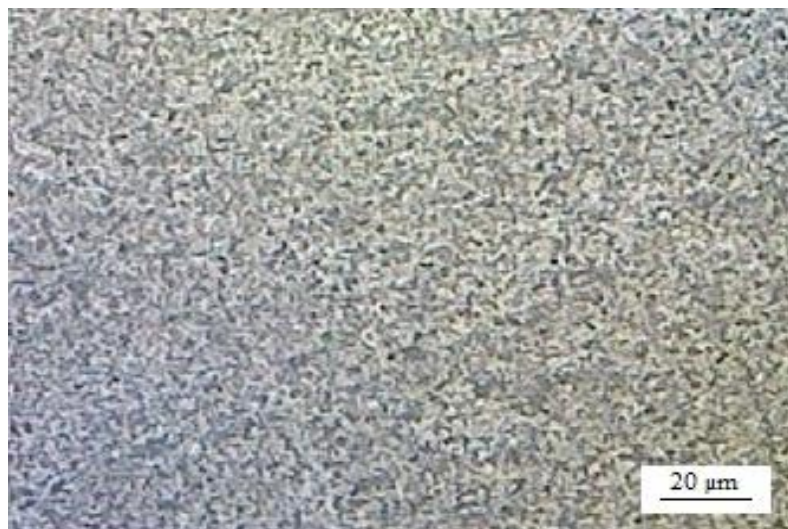


Figure No. 15 (b) Microstructure of the one pass FSPed specimen cross section



Figure No. 15 (c) Microstructure of the two pass FSPed specimen cross section



Figure No. 15 (d) Microstructure of the three pass FSPed specimen cross section



Figure No. 15 (e) Microstructure of the four pass FSPed specimen cross section

#### 4.2 Micro-hardness:-

The micro-hardness samples are prepared by machining of 1mm top surface and the samples are checked. The micro-hardness measurement on the sample was done using micro-hardness tester under the load of 0.5kg with a dwell time of 10sec. The detailed micro-hardness values are shown in figure no16

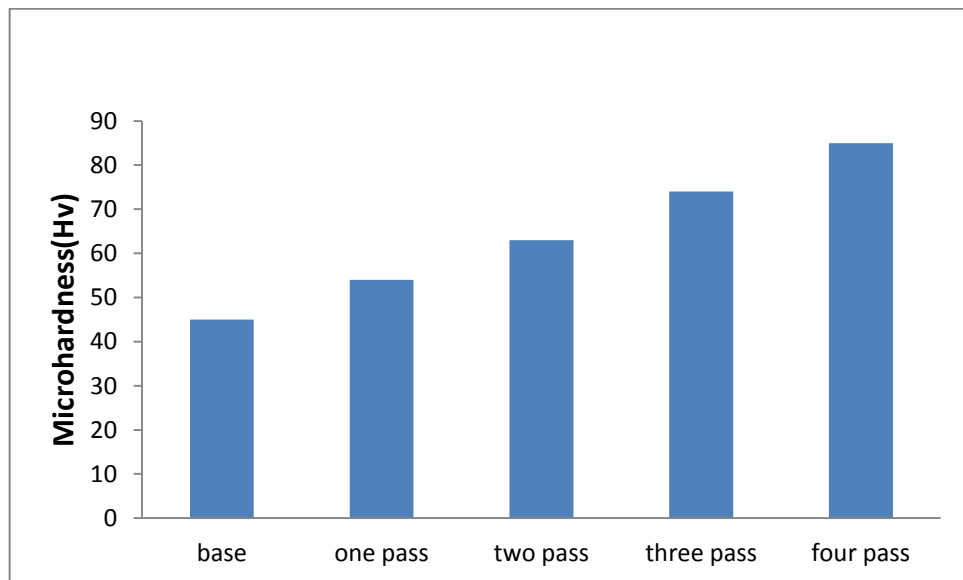


Figure No. 16 Micro-hardness of FSPed specimens on the top surface

The micro-hardness of samples was increased with increasing number of passes due to stirring of the processed material and refining of grain size.

### 4.3 Tensile data:-

Table 4 Tensile results of all specimens:

Experiment no.	Tensile Strength (MPa)
1	106
2	117
3	82
4	103
5	60

### 4.4 Stress V/s Strain diagrams:-

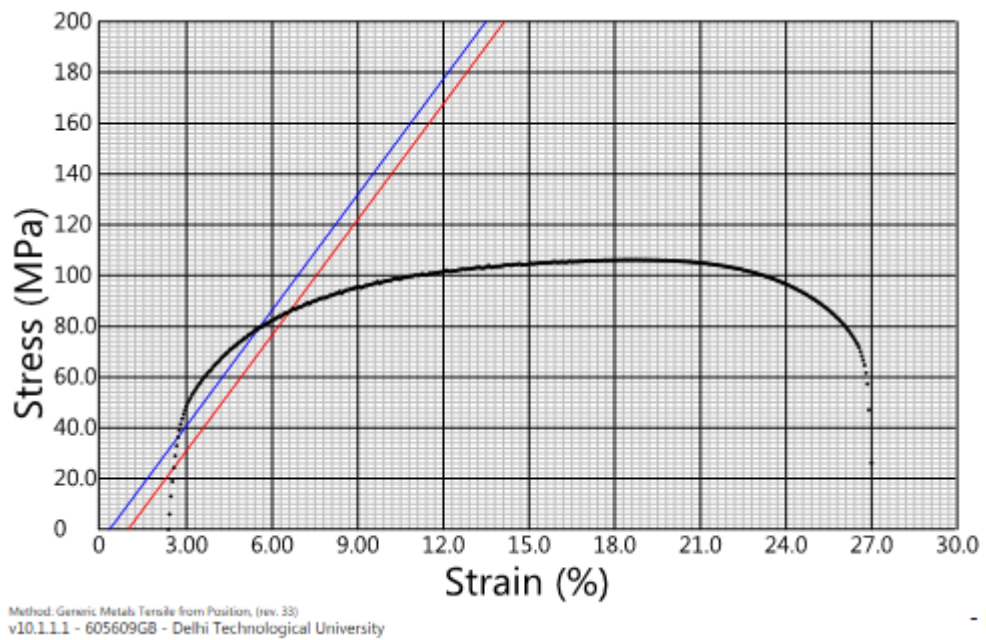


Figure No. 17 (a) Tensile specimen of base material sample

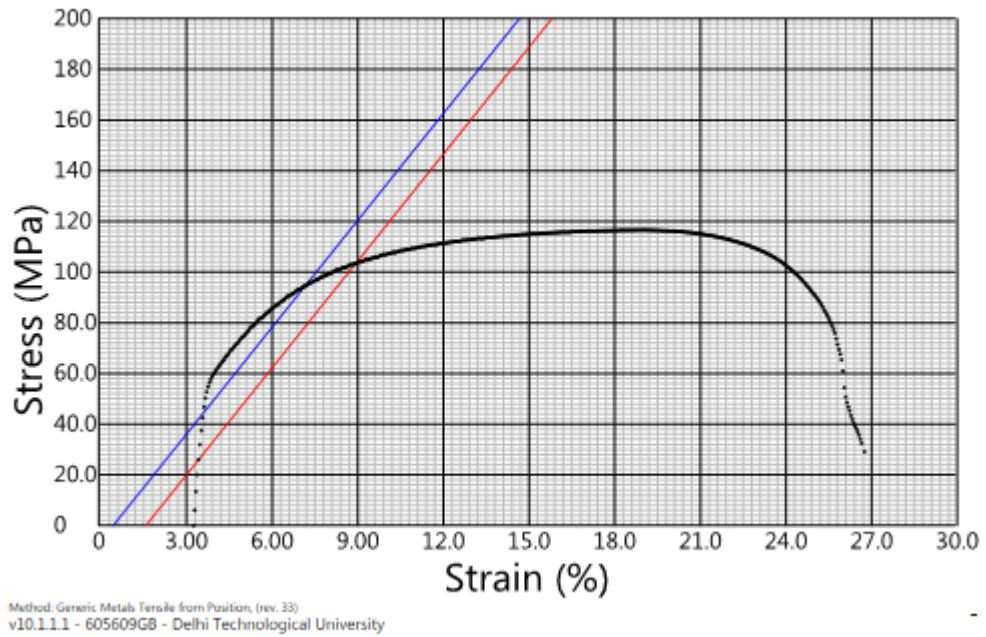


Figure No. 17 (b) Tensile specimen of one pass FSPed sample

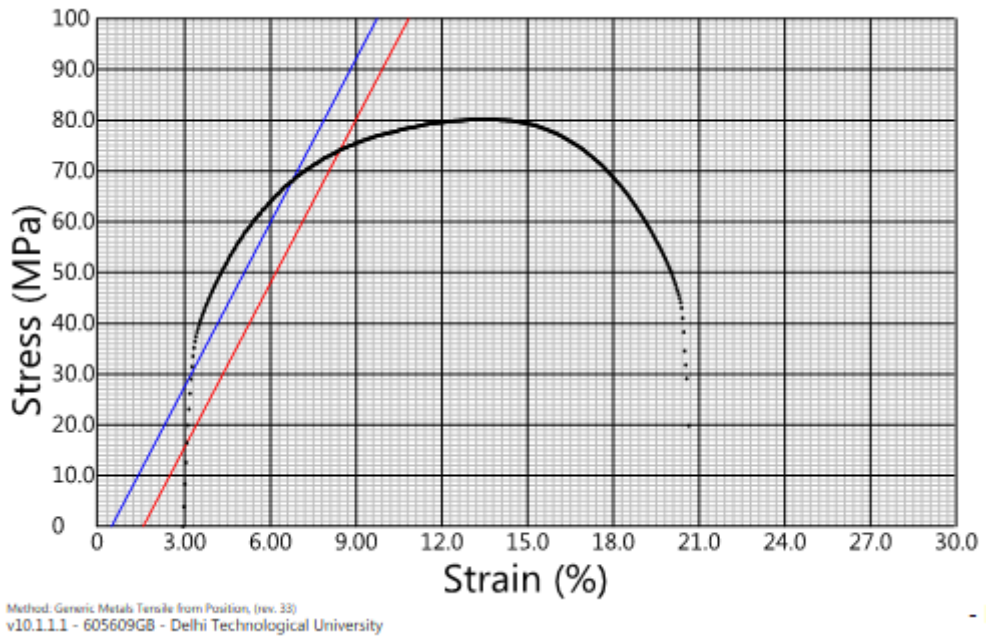


Figure No. 16 (c) Tensile specimen of two pass FSPed sample

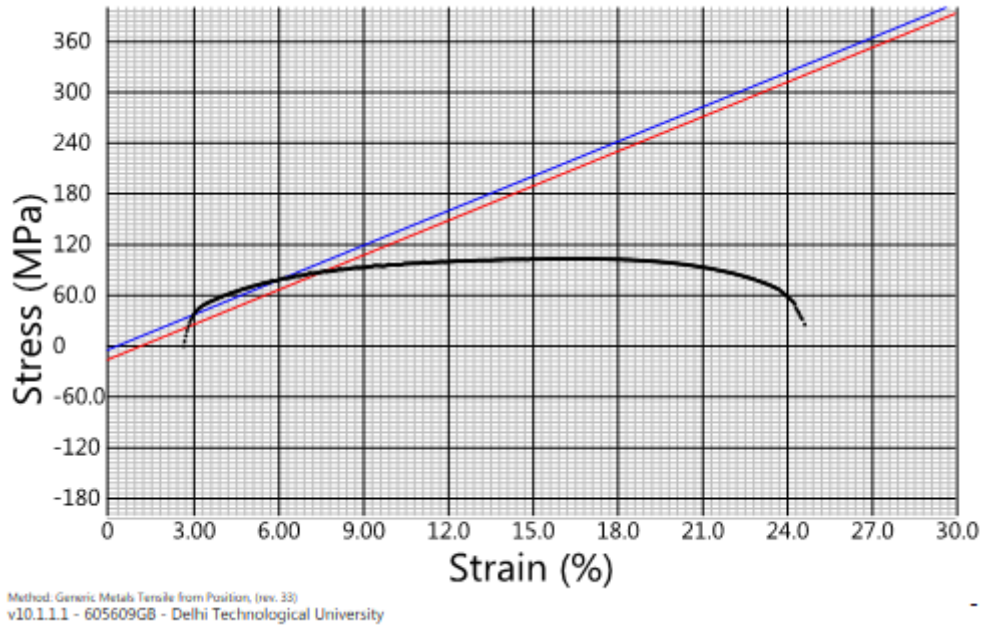


Figure No. 17 (d) Tensile specimen of three pass FSPed sample

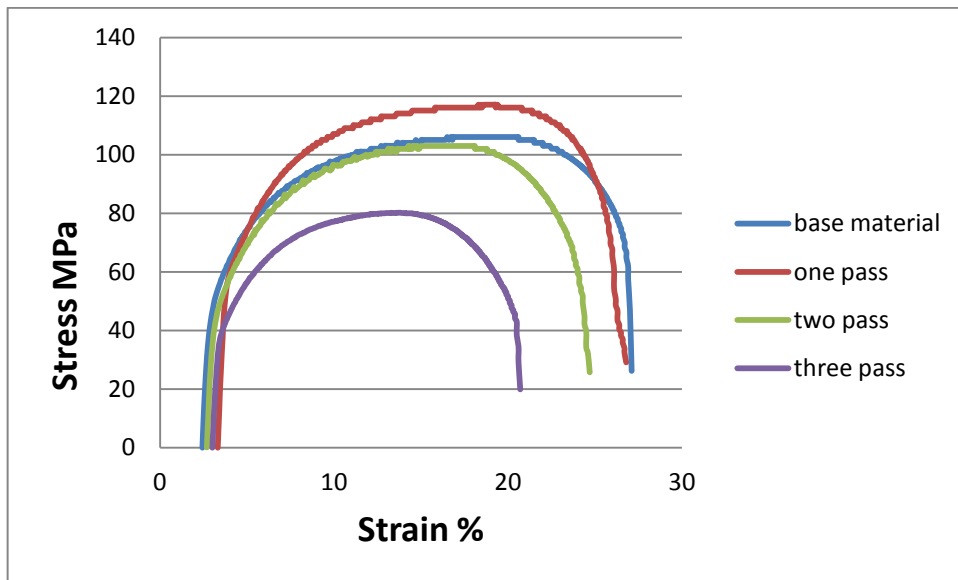


Figure No. 17 (e) Tensile specimen of FSPed Sample with different passes

## 4.5 Fractography of tensile specimens:-

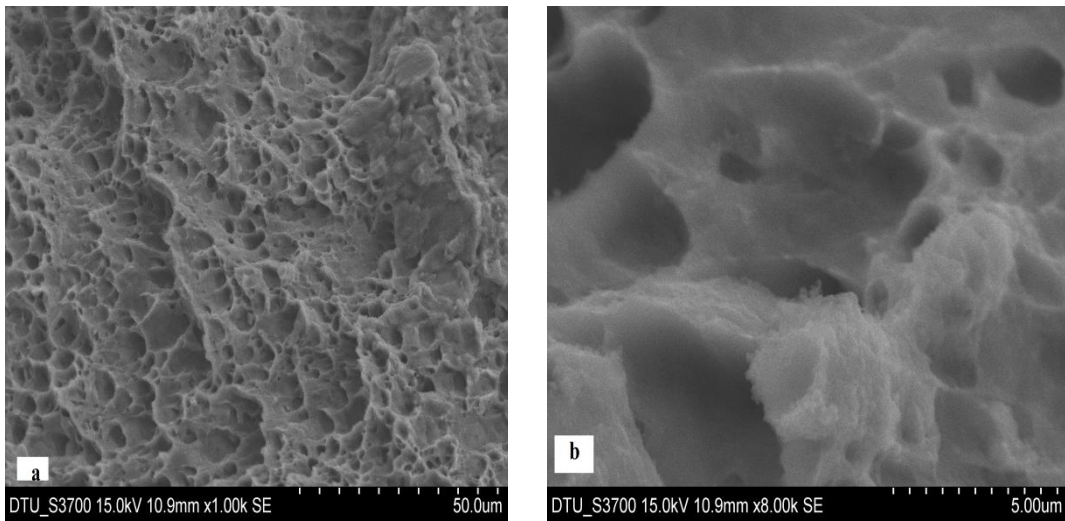


Figure No. 18 (a & b) Base material specimen tensile fractography (lower & higher magnification)

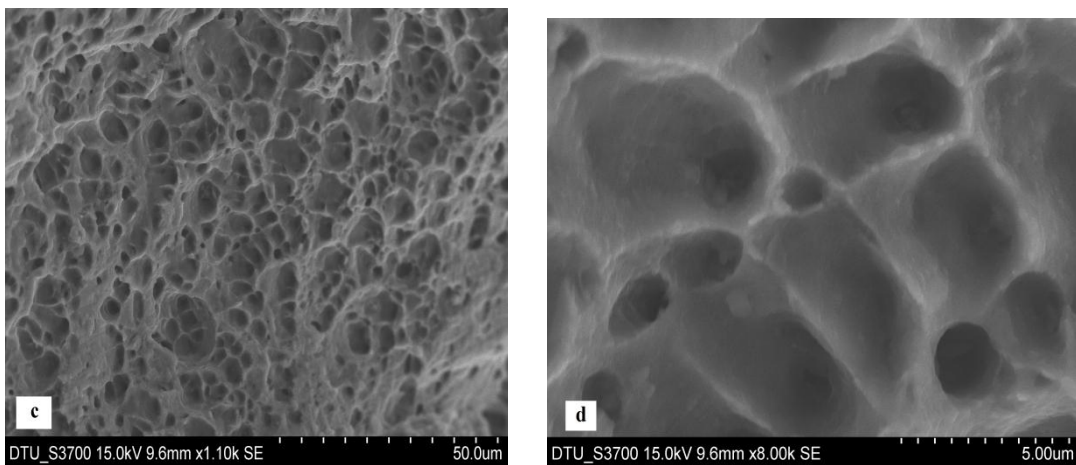


Figure No. 18 (c & d) FSPed one pass specimen tensile fractography (lower & higher magnification)



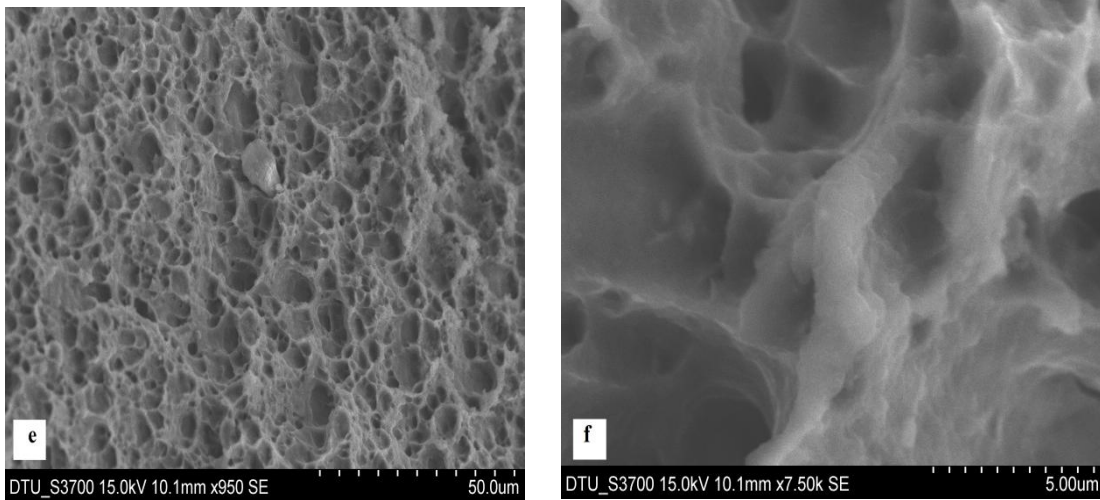


Figure No. 18 (e & f) FSPed two pass specimen tensile fractography (lower & higher magnification)

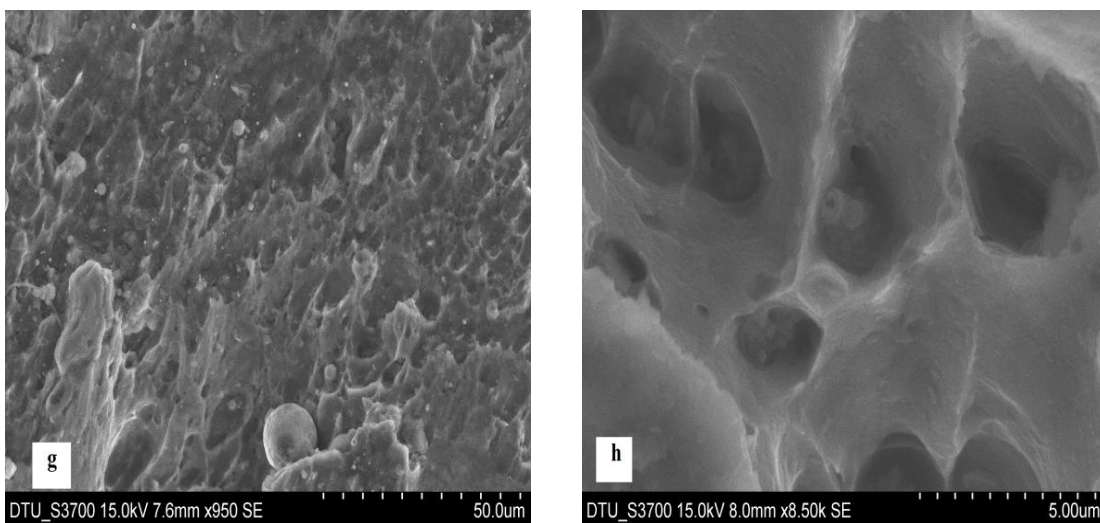


Figure No. 18 (g & h) FSPed three pass specimen tensile fractography (lower & higher magnification)

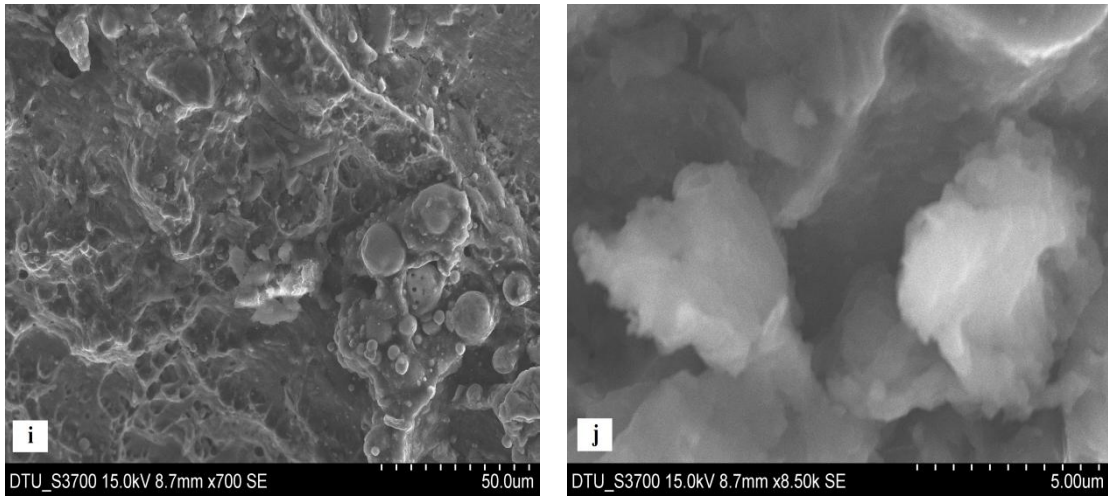


Figure No. 18 (i & j) FSPed four pass specimen tensile fractography (lower & higher magnification)

# CHAPTER-5

## Wear properties

---

### 5.1 wear rate:-

Table 5 Wear rate result for base material specimen:

Weight		mass difference (gm)	cumulative mass difference (gm)	Sliding Distance (m)	wear rate (gm/m)
Before wear(gm)	After wear (gm)				
20.1536	20.1536	0.0	0.0	0	0
20.1536	20.1455	0.0081	0.0081	500	$1.62 \times 10^{-5}$
20.1455	20.1372	0.0083	0.0164	1000	$1.64 \times 10^{-5}$
20.1372	20.1287	0.0085	0.0249	1500	$1.66 \times 10^{-5}$
20.1287	20.1201	0.0086	0.0335	2000	$1.67 \times 10^{-5}$
20.1201	20.1118	0.0083	0.0418	2500	$1.67 \times 10^{-5}$
20.1118	20.1031	0.0087	0.0505	3000	$1.68 \times 10^{-5}$

Table 6 Wear rate result for FSPed one pass specimen:

Weight		mass difference (gm)	cumulative mass difference (gm)	Sliding Distance (m)	wear rate (gm/m)
before wear(gm)	after wear (gm)				
19.8815	19.8815	0.0	0.0	0	0
19.8815	19.8751	0.0064	0.0064	500	$1.28 \times 10^{-5}$
19.8751	19.8685	0.0066	0.013	1000	$1.3 \times 10^{-5}$
19.8685	19.8618	0.0067	0.0197	1500	$1.31 \times 10^{-5}$
19.8618	19.855	0.0068	0.0265	2000	$1.33 \times 10^{-5}$
19.855	19.8481	0.0069	0.0334	2500	$1.34 \times 10^{-5}$
19.8481	19.8411	0.007	0.0404	3000	$1.35 \times 10^{-5}$

Table 7 Wear rate result for FSPed two pass specimen:

Weight		mass difference (gm)	cumulative mass difference (gm)	Sliding Distance (m)	wear rate (gm/m)
before wear(gm)	after wear (gm)				
20.5169	20.5169	0.0	0.0	0	0
20.5169	20.5115	0.0054	0.0054	500	$1.08 \times 10^{-5}$
20.5115	20.506	0.0055	0.0109	1000	$1.09 \times 10^{-5}$
20.506	20.5002	0.0058	0.0167	1500	$1.11 \times 10^{-5}$
20.5002	20.4942	0.0060	0.0227	2000	$1.13 \times 10^{-5}$
20.4942	20.4883	0.0059	0.0286	2500	$1.14 \times 10^{-5}$
20.4883	20.4823	0.0060	0.0346	3000	$1.15 \times 10^{-5}$

Table 8 Wear rate result for FSPed three pass specimen:

Weight		mass difference (gm)	cumulative mass difference (gm)	Sliding Distance (m)	wear rate (gm/m)
before wear(gm)	after wear (gm)				
20.4413	20.4413	0.0	0.0	0	0
20.4413	20.4363	0.0050	0.0050	500	$1.00 \times 10^{-5}$
20.4363	20.4311	0.0052	0.0102	1000	$1.02 \times 10^{-5}$
20.4311	20.4258	0.0053	0.0155	1500	$1.033 \times 10^{-5}$
20.4258	20.4207	0.0051	0.0206	2000	$1.03 \times 10^{-5}$
20.4207	20.4155	0.0052	0.0258	2500	$1.032 \times 10^{-5}$
20.4155	20.4104	0.0051	0.0309	3000	$1.03 \times 10^{-5}$

Table 9 Wear rate result for FSPed four pass specimen:

Weight		mass difference (gm)	cumulative mass difference (gm)	Sliding Distance (m)	wear rate (gm/m)
before wear(gm)	after wear (gm)				
20.7383	20.7383	0.0	0.0	0	0
20.7383	20.734	0.0043	0.0043	500	$8.6 \times 10^{-6}$
20.734	20.7295	0.0045	0.0088	1000	$8.8 \times 10^{-6}$
20.7295	20.7249	0.0046	0.0134	1500	$8.933 \times 10^{-6}$
20.7249	20.7202	0.0047	0.0181	2000	$9.05 \times 10^{-6}$
20.7202	20.7154	0.0048	0.0229	2500	$9.16 \times 10^{-6}$
20.7154	20.7107	0.0047	0.0276	3000	$9.2 \times 10^{-6}$

## 5.2 wear rate v/s sliding distance:-

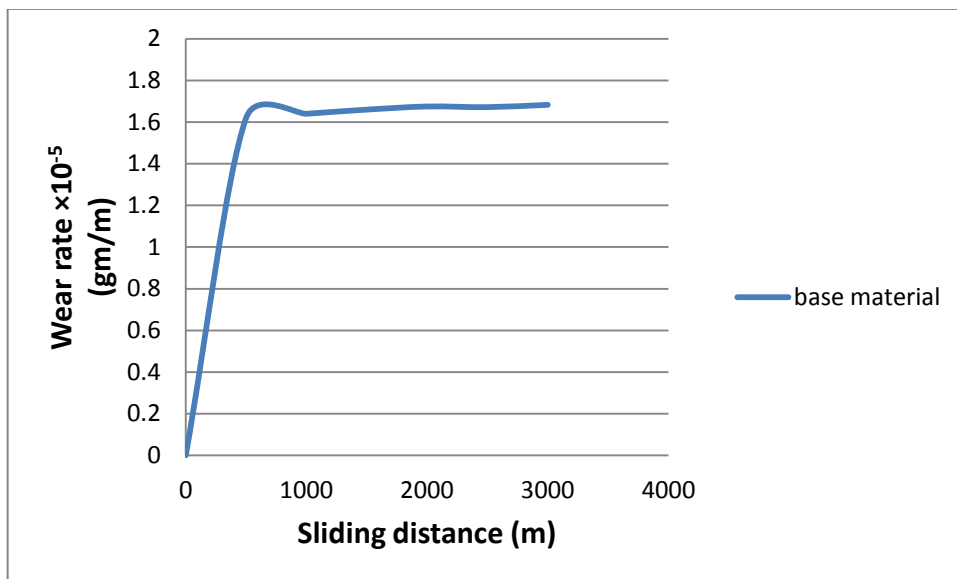


Figure No. 19 (a) wear rate of the base material specimen

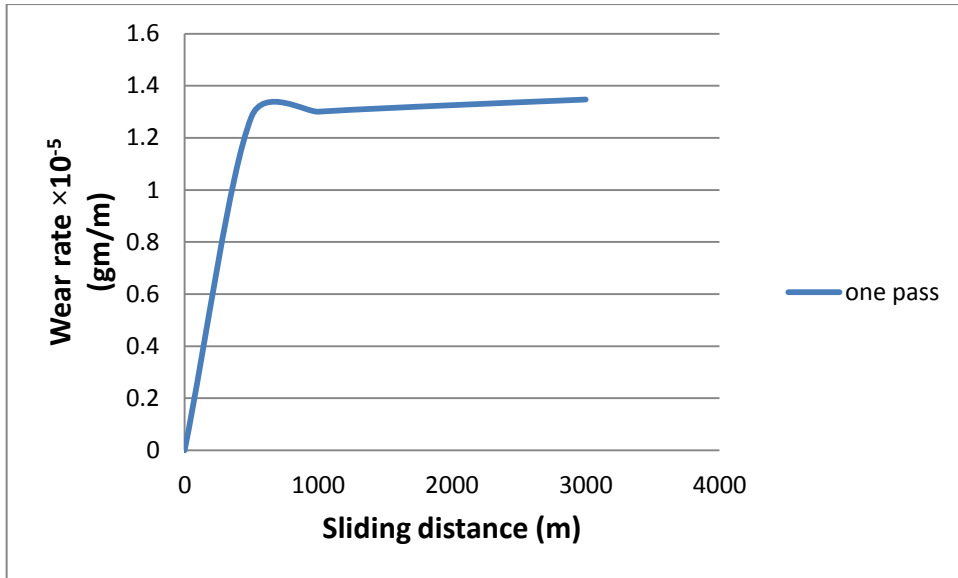


Figure No. 19 (b) wear rate of the one pass FSPed specimen

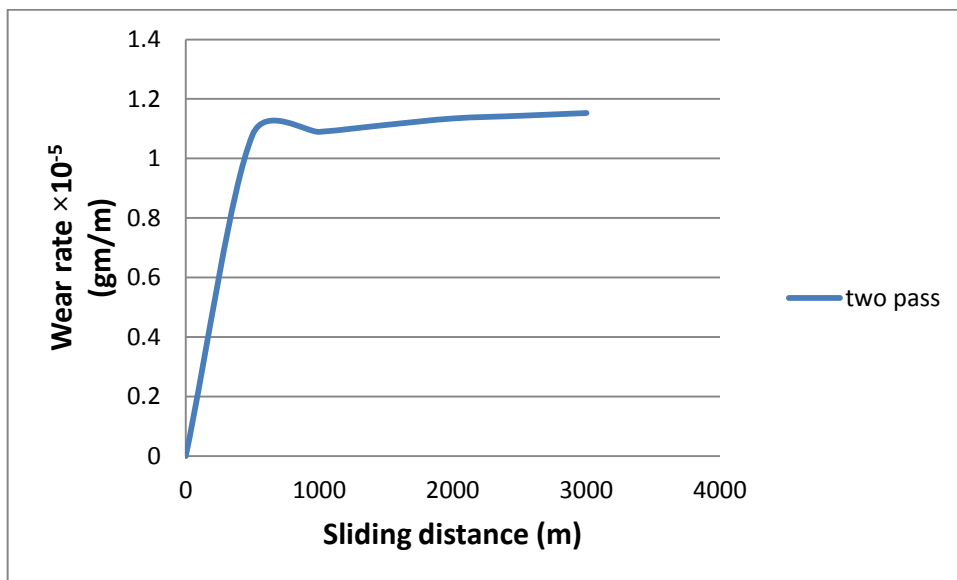


Figure No. 19 (c) wear rate of the two pass FSPed specimen

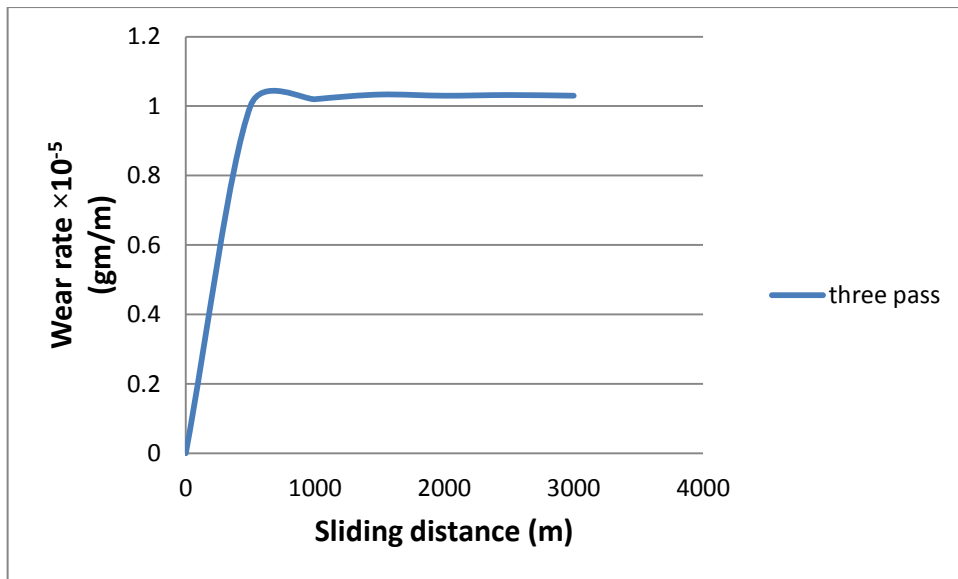


Figure No. 19 (d) wear rate of the three pass FSPed specimen

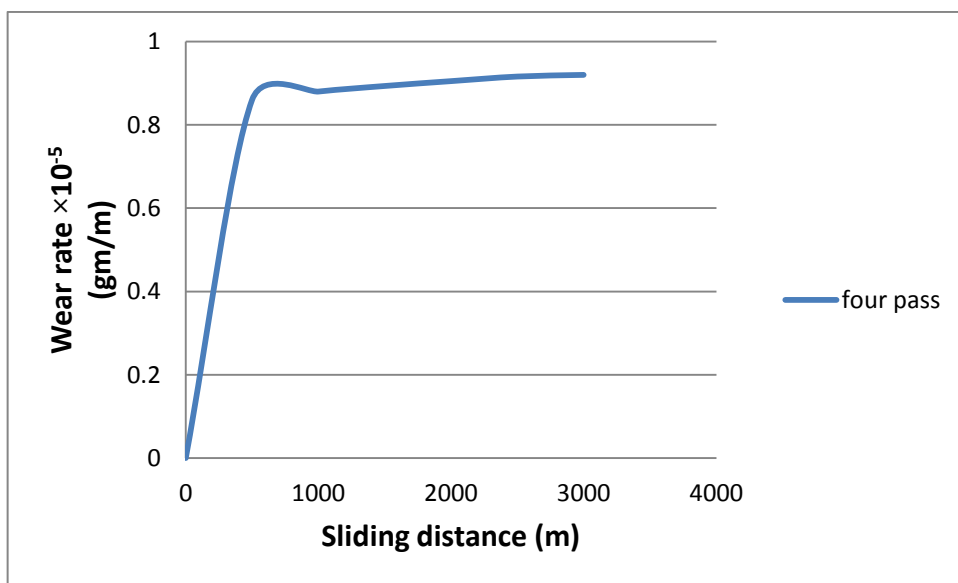


Figure No. 19 (e) wear rate of the four pass FSPed specimen

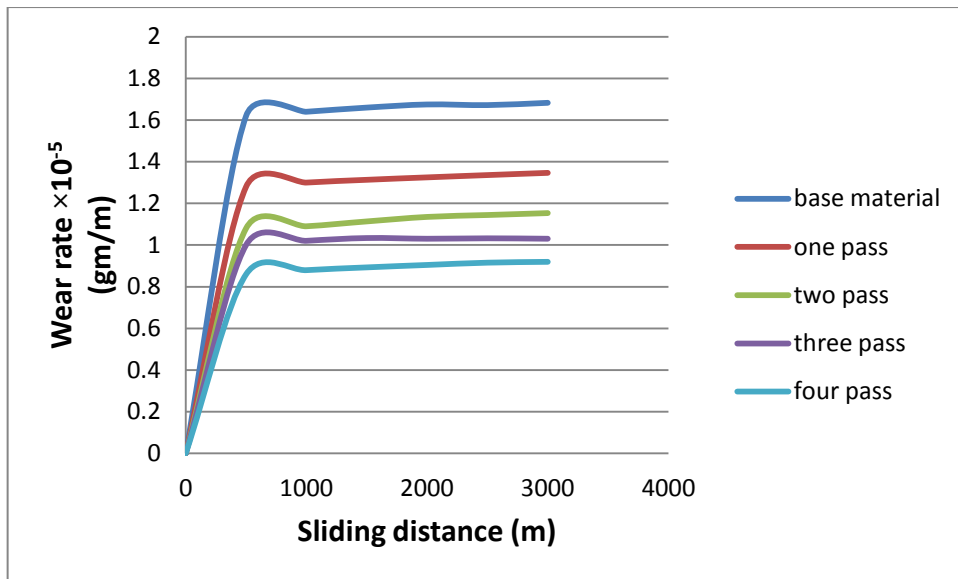


Figure No. 19 (f) wear rate of the FSPed specimen with different passes

### 5.3 Friction coefficient v/s sliding distance:-

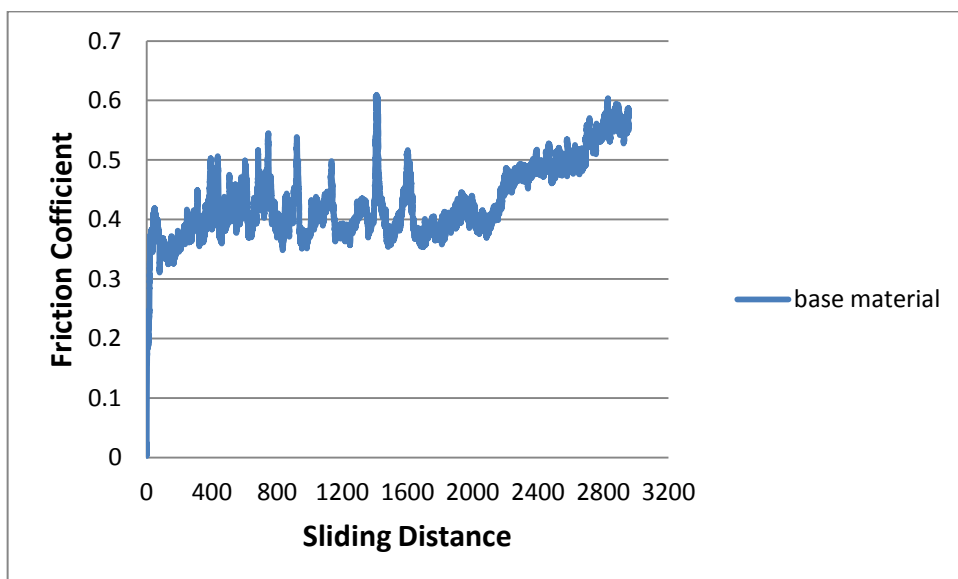


Figure No. 20 (a) base material



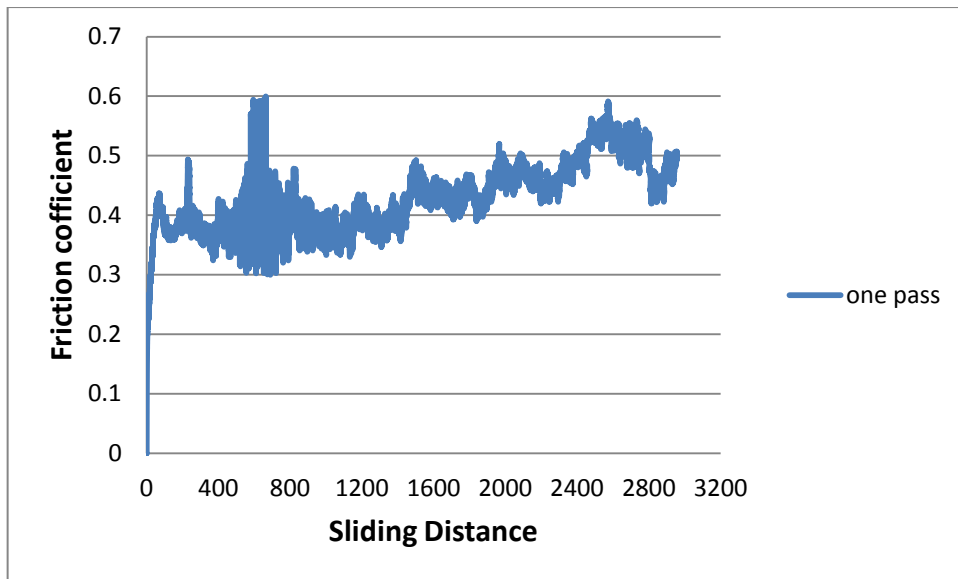


Figure No. 20 (b) one pass processed material

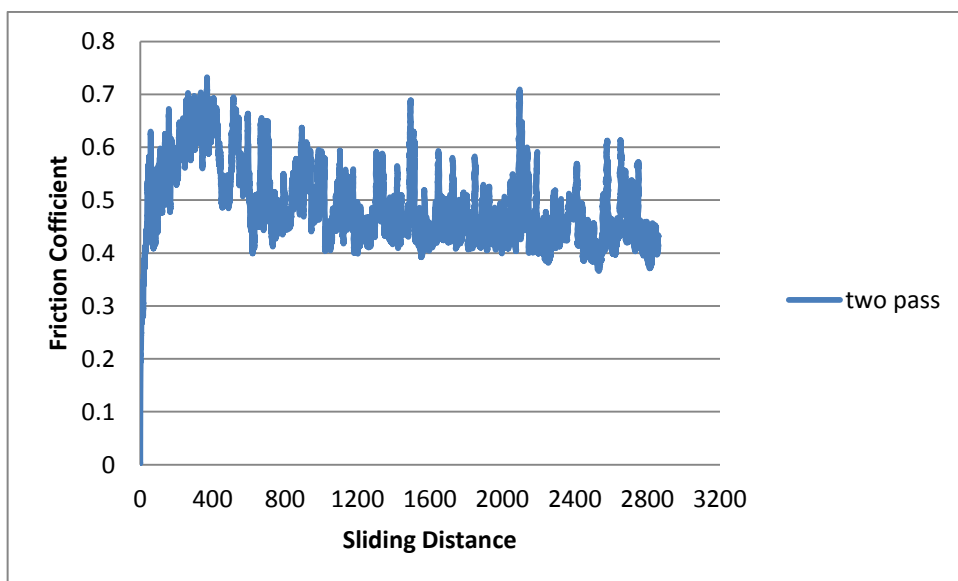


Figure No. 20 (c) two pass processed material

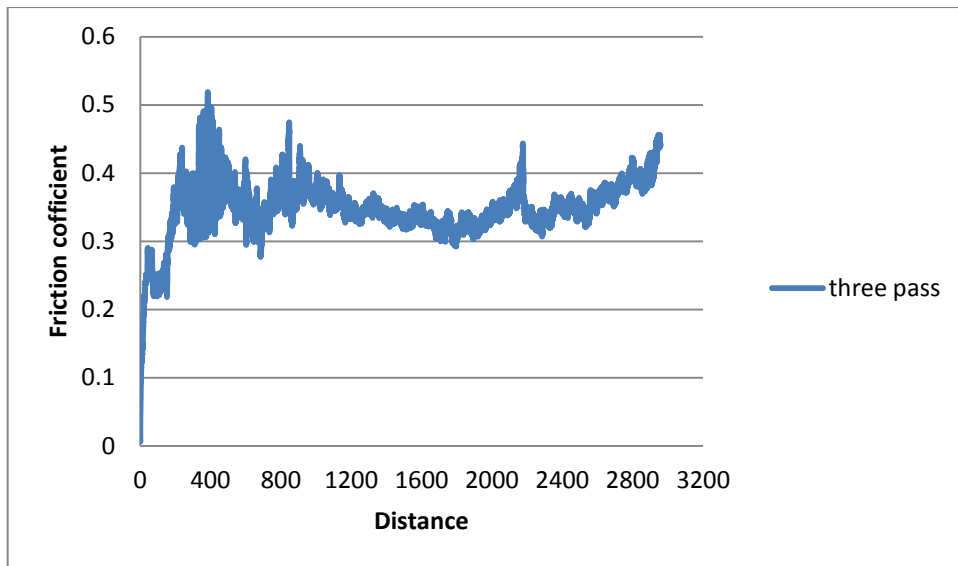


Figure No. 20 (d) three pass processed material

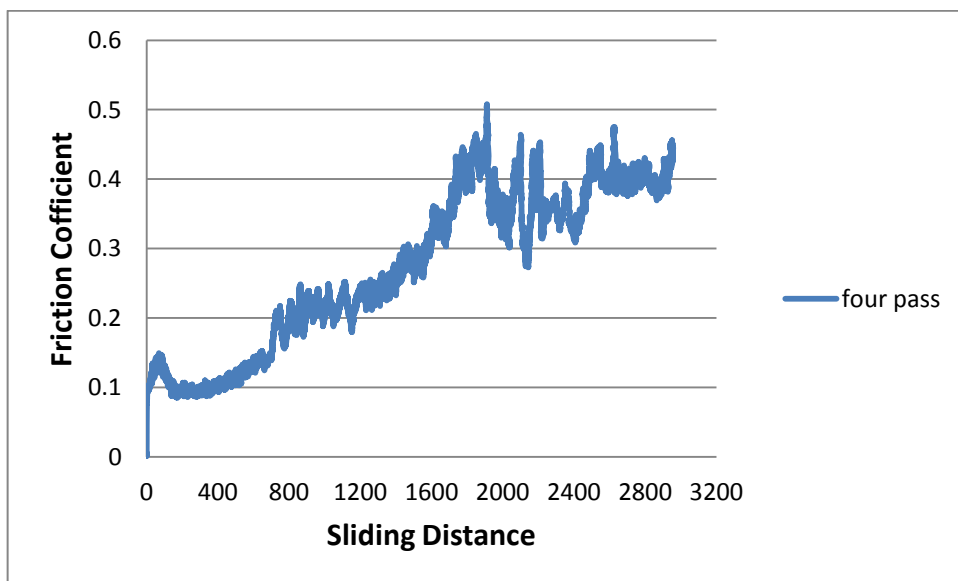


Figure No. 20 (e) four pass processed material

## 5.4 SEM of wear test specimen:-

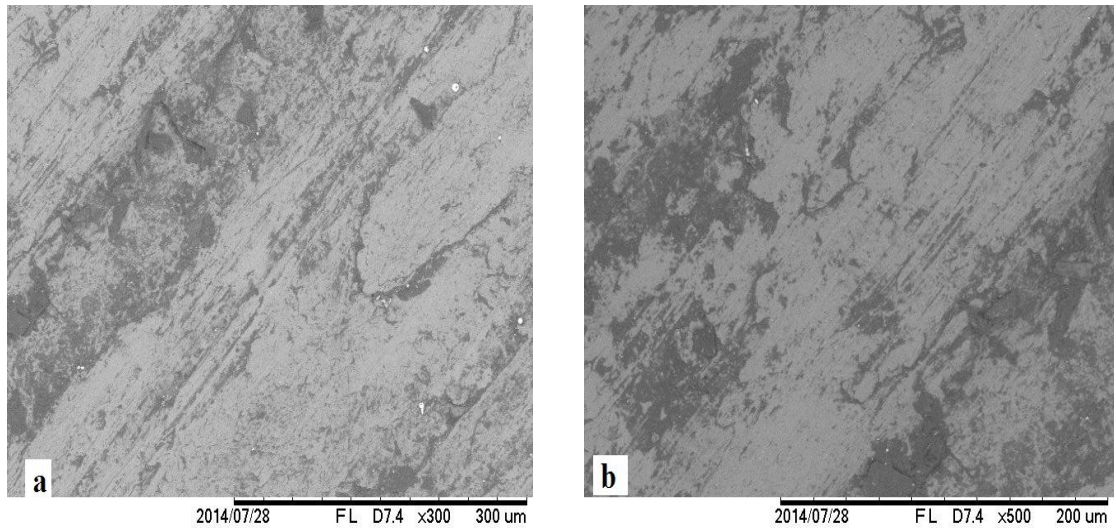


Figure No. 21 (a & b) Base material wear test specimen (lower & higher magnification)

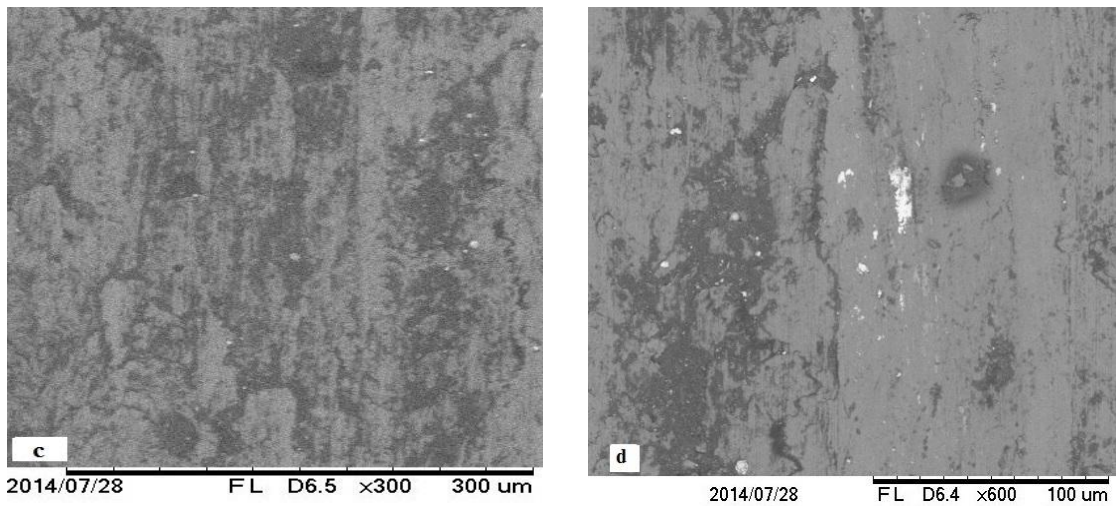


Figure No. 21 (c & d) FSPed one pass wear test specimen (lower & higher magnification)

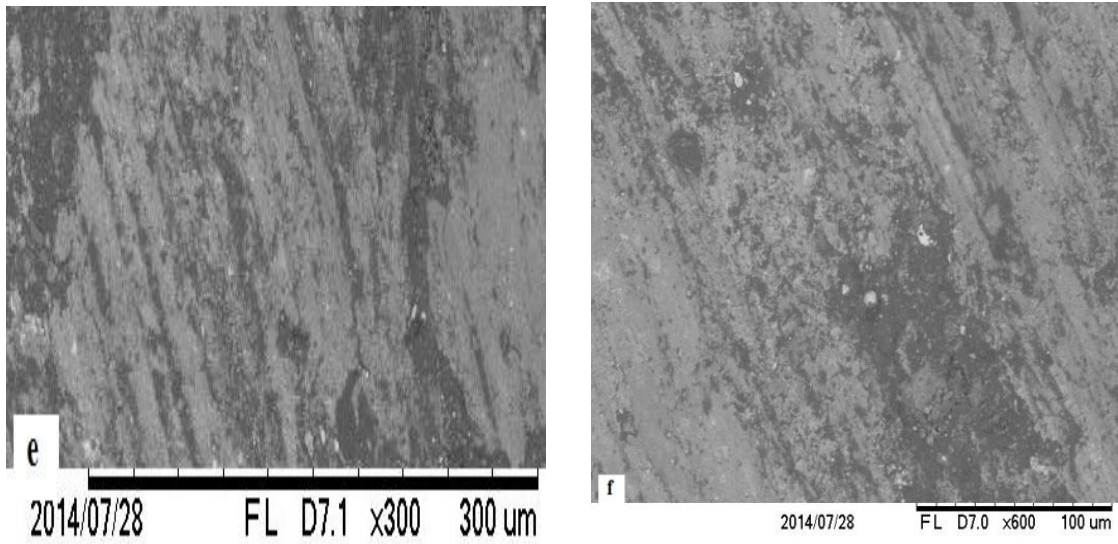


Figure No. 21 (e & f) FSPed two pass wear test specimen (lower & higher magnification)

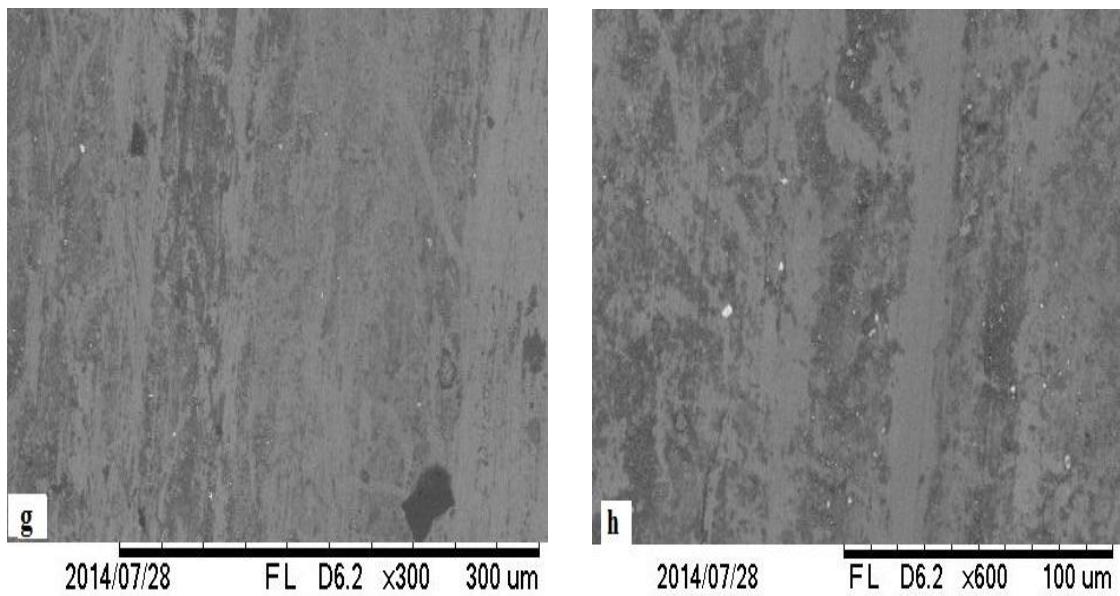


Figure No. 21 (g & h) FSPed three pass wear test specimen (lower & higher magnification)

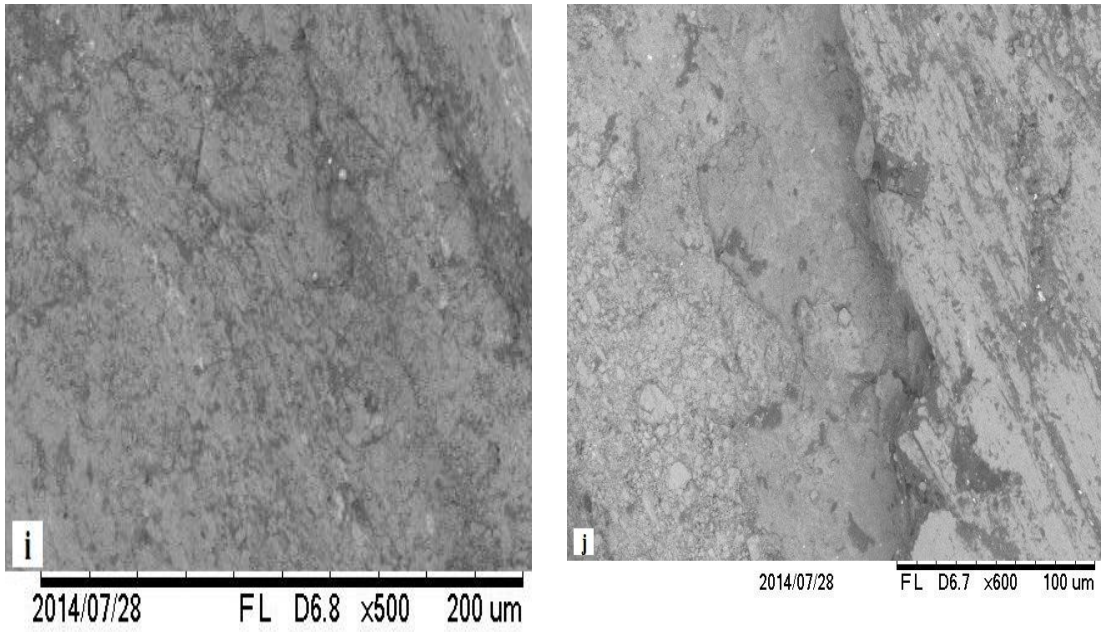


Figure No. 21 (i & j) FSPed four pass wear test specimen (lower & higher magnification)

## 5.5 Temperature distribution over friction disc:-

Table 10 Image Information about FSPed one pass specimen:-

Background temperature	25.0°C
Emissivity	0.95
Transmission	1.00
Average Temperature	32.8°C
Image Range	31.2°C to 54.1°C
Camera Model	Ti400
IR Sensor Size	320 x 240
Camera serial number	Ti400-13120004
Camera Manufacturer	Fluke Thermography
Image Time	5/26/2014 2:31:21 PM
Calibration Range	-20.0°C to 250.0°C

Name	Temperature	Emissivity	Background
Center point	34.7°C	0.95	25.0°C
Hot	54.1°C	0.95	25.0°C
Cold	31.2°C	0.95	25.0°C
P0	37.5°C	0.95	25.0°C

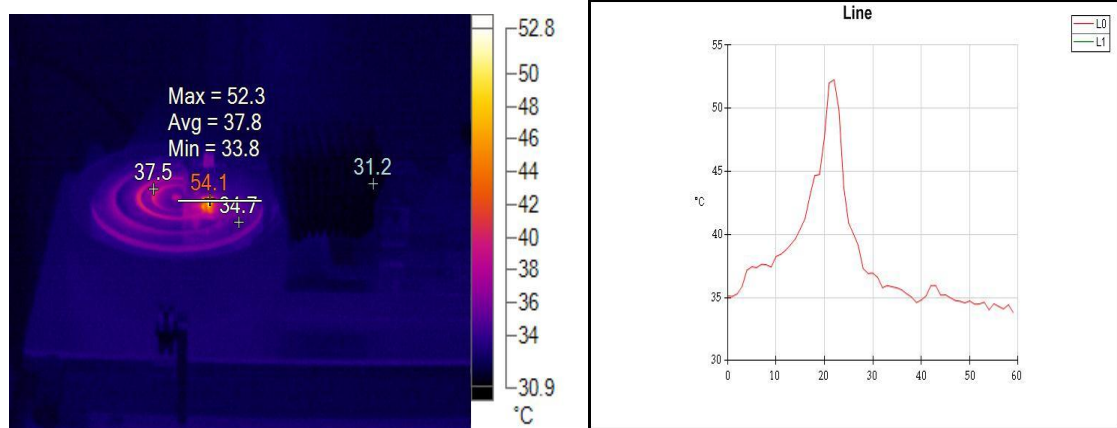


Figure No. 22 (a) temperature variation of two pass FSPed sample with sliding distance during wear testing

**Table 11 Image Information about three pass sample:-**

Background temperature	25.0°C
Emissivity	0.95
Transmission	1.00
Average Temperature	34.9°C
Image Range	31.9°C to 66.5°C
Camera Model	Ti400
IR Sensor Size	320 x 240
Camera serial number	Ti400-13120004
Camera Manufacturer	Fluke Thermography
Image Time	5/27/2014 12:12:26 PM
Calibration Range	-20.0°C to 250.0°C

Name	Temperature	Emissivity	Background
Center point	34.2°C	0.95	25.0°C
Hot	66.5°C	0.95	25.0°C
Cold	31.9°C	0.95	25.0°C
P0	35.4°C	0.95	25.0°C

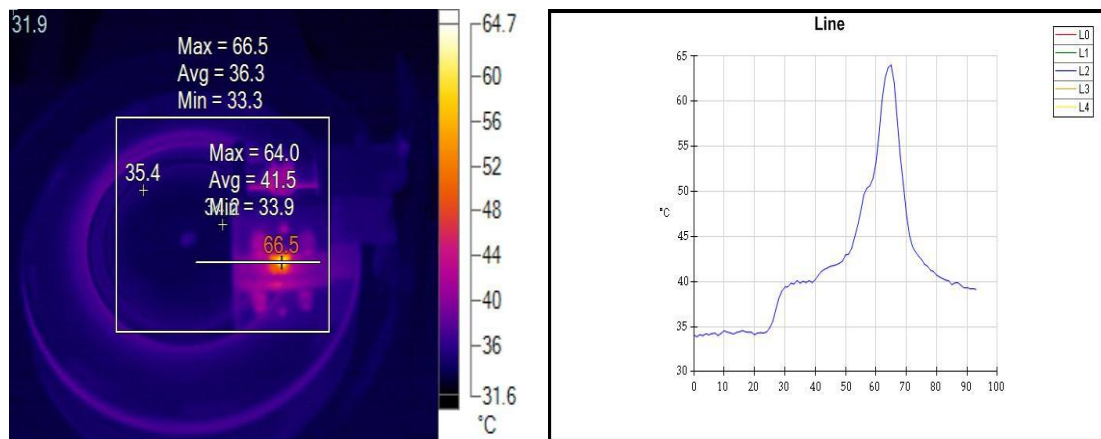


Figure No. 22 (b) temperature variation of tree pass FSPed sample with sliding distance during wear testing

# CHAPTER-6

---

## Conclusions:-

In the present research work we successfully processed the surface of AA1050 aluminium alloy at 1600rpm and 25mm/min with square pin profile tool of H-13 tool material with different passes and studied the microstructure, tensile properties, and micro-hardness and wear behaviour of FSPed surface of aluminium alloy with different passes and compared with the properties of base material. This chapter summarise all the major observations and the conclusions drawn from this study as well as highlights the significant contributions of this thesis to the existing knowledge.

1. The grain size becomes finer of processed samples with increasing no passes compared to base material and one pass specimen.
2. The micro-hardness of four pass FSPed specimen (85Hv) is higher compare to one pass FSPed specimen (54Hv) and base material specimen (45Hv) of 1050 aluminium alloy.
3. The ultimate tensile strength (117MPa) of one pass FSPed processed sample is higher in compare to base material (106MPa). The ultimate tensile strength of processed samples increased with increasing the number of passes compared to base material.
4. The percentage elongations for processed samples are one pass (26.5%), two pass (20.5%), three pass (18%) and four pass (17%). With increasing the no of passes the percentage tensile elongation is decreased in compare to base material (26.8) samples.
5. The hardness of processed samples increase with increasing no of passes compared to without processed samples.
6. The average coefficient of friction decrease with increasing no of passes for same loading 40N.
7. Wear rate of processed samples decrease with increasing no of passes for same sliding distance 3000 meter and constant speed 261 rpm compared to base material samples.
8. Average temperature on the disc of wear testing machine decrease with increasing number of passes for same track diameter, load 40N and speed 261 rpm.



## REFERENCES

1. Thomas W.M, Nicholas E.D, Needham J.C, Murch M.G, Templesmith P, Dawes C.J, “Friction-stir butt welding” G.B. Patent Application No. 9125978.8 (December1991).
2. Ehab A. El-Danaf, Magdy M. El-Rayes, “Microstructure and mechanical properties of friction stir welded 6082 AA inas welded and post weld heat treated conditions” *Materials and Design* 46 (2013) 561–572
3. R.S. Mishra, Z.Y. Ma, “Friction stir welding and processing” *Materials Science and Engineering*50 (2005) 1–78.
4. Ron Cobden, Alcan, “Banbury Aluminium: Physical Properties, Characteristics and Alloys” TALAT 1501 European Aluminium Association (1994).
5. Mishra R.S, Johannes L.B “Multiple passes of friction stir processing for thecreation of super-plastic 7075 aluminium” *Materials Science and Engineering A* 464 (2007) 255–260
6. Barmouz M, Givi M.K.B “Fabrication of in situ Cu/SiC composites using multi-pass friction stir processing: Evaluation of micro-structural, porosity, mechanical and electrical behavior” *Composites: Part A* 42 (2011) 1445–1453
7. Brown R, Tang W, Reynolds A.P “Multi-pass friction stir welding in alloy 7050-T7451: Effects on weld response variables and on weld properties” *Materials Science and Engineering A* 513–514 (2009) 115–121
8. Rao A.G, Katkar V.A, Gunasekaran G, Deshmukh V.P, Prabhu N, Kashyap B.P “Effect of multipass friction stir processing on corrosion resistance of hypereutectic Al–30Si alloy” *Corrosion Science* 83 (2014) 198–208
9. Ma Z.Y, Mishra R.S, Liu F.C “Super-plastic behaviour of micro-regions in two-pass friction stir processed 7075Al alloy” *Materials Science and Engineering A* 505 (2009) 70–78
10. Ma Z.Y, Sharma S.R, Mishra R.S “Effect of multiple-pass friction stir processing on microstructure and tensile properties of a cast aluminium–silicon alloy” *Scripta Materialia* 54 (2006) 1623–1626
11. Devaraju A, Kumar A, Kotiveerachari B, “Influence of rotational speed and reinforcement on wear & mechanical Properties of aluminium hybrid composites via FSP” *Materials and Design* 45(2013)576–585.

12. Murtha S.J, "New 6xxx aluminium alloy for automotive body sheet applications" SAE International Journal of Materials Manufacturing, 104 (1995), 657–666.
13. Shen Z, Yang X, Zhang Z, Cui L, Yin Y "Mechanical properties and failure mechanisms of friction stir spot welds of AA 6061-T4 sheets" Materials and Design 49 (2013) 181–191
14. Choi D.H,Ahn B.W, Quesnel D.J, Jung S.B " "Behaviour of  $\beta$  phase ( $Al_3Mg_2$ )in AA 5083 during friction stir welding" Inter-metallic's 35 (2013) 120-127
15. El-Danaf E.A, El-Rayes M.M "Microstructure and mechanical properties of friction stir welded 6082 AA in as welded and post weld heat treated conditions" Materials and Design 46 (2013) 561–572
16. Li J.Q, Liu H.J "Characteristics of the reverse dual-rotation friction stir welding conducted on 2219-T6 aluminium alloy" Materials and Design 45 (2013) 148–154
17. Rao D, Huber K, Heerens J, dosSantos J.F, Huber N. "Asymmetric mechanical properties and tensile behaviour prediction of aluminium alloy 5083 friction stir welding joints" Materials Science & Engineering A 565 (2013) 44–50
18. Shen Z, Yang X, Zhang Z, Cui L, Li T. "Microstructure and failure mechanisms of refill friction stir spot welded 7075-T6 aluminium alloy joints" Materials and Design 44 (2013) 476–486
19. Bisadi H, Tavakoli A, Sangsaraki M.T, Sangsaraki K.T "The influences of rotational and welding speeds on microstructures and mechanical properties of friction stir welded Al5083 and commercially pure copper sheets lap joints" Materials and Design 43 (2013) 80–88
20. Sharma C, Dwived D.K, Kumar P. "Effect of post weld heat treatments on microstructure and mechanical properties of friction stir welded joints of Al–Zn–Mg alloy AA7039" Materials and Design 43 (2013) 134–143
21. Feng X, Liub H, Lippolda J.C "Microstructure characterization of the stir zone of submerged friction stir processed aluminium alloy 2219" Materials characterization 82 ( 2 0 1 3 ) 9 7 – 1 0 2
22. Zhang Q., Xiao B.L, Wang Q.Z, Ma Z.Y "In situ  $Al_3Ti$  and  $Al_2O_3$  nanoparticles reinforced Al composites produced by friction stir processing in an Al–TiO<sub>2</sub> system" Materials Letters 65 (2011) 2070–2072

23. Rejil C.M, Dinaharan I, Vijay S.J, Murugan N. “Microstructure and sliding wear behaviour of AA6360/(TiC + B4C) hybrid surface composite layer synthesized by friction stir processing on aluminium substrate” *Materials Science and Engineering A* 552 (2012) 336– 344
24. Hao H.L, Ni D.R, Huang H, Wang D, Xiao B.L, Nie Z.R, Ma Z.Y “Effect of welding parameters on microstructure and mechanical properties of friction stir welded Al–Mg–Er alloy” *Materials Science & Engineering A* 559 (2013) 889–896
25. Badarinarayan H, Yang Q, Zhu S. “Effect of tool geometry on static strength of friction stir spot-welded aluminium alloy” *International Journal of Machine Tools & Manufacture* 49 (2009) 142–148
26. El-Rayesa M.M, El-Danaf E.A, “The influence of multi-pass friction stir processing on the micro-structural and mechanical properties of Aluminium Alloy 6082” *Journal of Materials Processing Technology* 212 (2012) 1157–1168
27. Al-Fadhalah K.J, Almazrouee A.I, Aloraier A.S “Microstructure and mechanical properties of multi-pass friction stir processed aluminium alloy 6063” *Materials and Design* 53 (2014) 550–560
28. Elangovan K., Balasubramanian V. “Influences of pin profile and rotational speed of the tool on the formation of friction stir processing zone in AA2219 aluminium alloy ” *Materials Science and Engineering A* 459 (2007) 7–18
29. Balasubramanian V., Elangovan K. “Influences of tool pin profile and tool shoulder diameter on the formation of friction stir processing zone in AA6061 aluminium alloy” *Materials and Design* 29 (2008) 362–373
30. Nascimento F., Santos T., Vilaca P, Miranda R.M, Quintino L. “Microstructural modification and ductility enhancement of surfaces modified by FSP in aluminium alloys” *Materials Science and Engineering A* 506 (2009) 16–22